

# European Journal of Agronomy

## Quantifying critical N dilution curves across $G \times E \times M$ effects for potato using a partially-pooled Bayesian hierarchical method

--Manuscript Draft--

<b>Manuscript Number:</b>	
<b>Article Type:</b>	Research paper
<b>Section/Category:</b>	Crop Physiology
<b>Keywords:</b>	critical nitrogen dilution curve; nitrogen nutrition index; nitrogen use efficiency; potato; Bayesian; genotype-by-environment-by-management interactions
<b>Corresponding Author:</b>	Brian Joseph Bohman, Ph.D. University of Minnesota Twin Cities: University of Minnesota Twin Cities UNITED STATES
<b>First Author:</b>	Brian Joseph Bohman, Ph.D.
<b>Order of Authors:</b>	Brian Joseph Bohman, Ph.D. Michael J. Culshaw-Maurer Ferial Ben Abdallah Claudia Giletto Gilles Bélanger Fabián G Fernández Yuxin Miao David J. Mulla Carl J. Rosen
<b>Abstract:</b>	Multiple critical N dilution curves [CNDs] have been previously developed for potato; however, attempts to directly compare differences in CNDs across genotype [G], environment [E], and management [M] interactions have been confounded by non-uniform statistical methods, biased experimental data, and lack of proper quantification of uncertainty in critical N concentration [%N <sub>c</sub> ]. This study implements a partially-pooled Bayesian hierarchical method to develop CNDs for previously published and newly reported experimental data, systematically evaluates the difference in %N <sub>c</sub> across $G \times E \times M$ effects, and directly compare CNDs from the Bayesian framework to CNDs from conventional statistical methods. The partially-pooled Bayesian hierarchical method implemented in this study has the advantage of being less susceptible to inferential bias at the level of individual $G \times E \times M$ interactions compared to alternative statistical methods which result from insufficient quantity and quality of experimental datasets (e.g., unbalanced distribution of N limiting and non-N limiting observations). This method also allows for a direct statistical comparison of differences in %N <sub>c</sub> [ $\Delta\%N_c$ ] across levels of the $G \times E \times M$ interactions. Where found to be significant, $\Delta\%N_c$ was attributed to variation in the timing of tuber initiation (e.g., maturity class) and the relative rate of tuber bulking (e.g., planting density) across $G \times E \times M$ interactions. In addition to using the median value for %N <sub>c</sub> (i.e., CND), the boundary values for the credible region (i.e., CND <sub>lo</sub> and CND <sub>up</sub> ) derived using the Bayesian framework should be used in calculation of N nutrition index (and other calculations) to account for and propagate uncertainty. Overall, this study provides additional evidence that %N <sub>c</sub> is dependent upon $G \times E \times M$ interactions; therefore, evaluation of crop N status or N use efficiency must account for variation in %N <sub>c</sub> across $G \times E \times M$ interactions.
<b>Suggested Reviewers:</b>	Ignacio Ciampitti ciampitti@ksu.edu Dr. Ciampitti has authored a number of studies on similar topics to this manuscript and would be an excellent reviewer/editor. Gilles Lemaire

	<p>gilles.lemaire.inra@gmail.com  Dr. Lemaire has authored a number of studies on similar topics to this manuscript and would be an excellent reviewer.</p>
	<p>David Makowski  makowski@grignon.inra.fr  Dr. Makowski has authored a number of studies on similar topics to this manuscript and would be an excellent reviewer.</p>
	<p>Javier Fernández  jafernandez@ksu.edu  Dr. Fernández has authored a number of studies on similar topics to this manuscript and would be an excellent reviewer.</p>
	<p>Victor Sadras  victor.sadras@sa.gov.au  Dr. Sadras has authored a number of studies on similar topics to this manuscript and would be an excellent reviewer.</p>

- Critical N dilution curves [CNCDs] for potato are subject to G x E x M effects
- Bayesian methods can quantify uncertainty in critical N concentration [%N<sub>c</sub>]
- Partial pooling Bayesian method enables direct comparison of G x E x M effects
- Variation in %N<sub>c</sub> for potato due to tuber initiation timing and tuber bulking rate
- N use efficiency and N nutrition index depend on %N<sub>c</sub> variability and uncertainty

**Quantifying critical N dilution curves across  $G \times E \times M$  effects for potato using a partially-pooled Bayesian hierarchical method**

Brian J. Bohman<sup>1</sup>, Michael J. Culshaw-Maurer<sup>2</sup>, Ferial Ben Abdallah<sup>3</sup>, Claudia Giletto<sup>4</sup>, Gilles Bélanger<sup>5</sup>, Fabián G., Fernández<sup>1</sup>, Yuxin Miao<sup>1</sup>, David J. Mulla<sup>1</sup>, and Carl J. Rosen<sup>1\*</sup>

1. Department of Soil, Water, and Climate, University of Minnesota. 1991 Upper Buford Circle, St. Paul MN 55108

2. CyVerse, University of Arizona.

3. Productions in Agriculture Department, Crop Production Unit, Walloon Agricultural Research Centre.

4. Unidad Integrada Balcarce, Facultad de Ciencias Agrarias (UNMdP)-INTA Balcarce. Ruta 226 km 73,5 (7620) Balcarce, Buenos Aires, Argentina

5. Science and Technology Branch, Agriculture and Agri-Food Canada, Québec City, Canada

\* Corresponding Author: rosen006@umn.edu

**Abstract:** Multiple critical N dilution curves [CNDCs] have been previously developed for potato; however, attempts to directly compare differences in CNDCs across genotype [G], environment [E], and management [M] interactions have been confounded by non-uniform statistical methods, biased experimental data, and lack of proper quantification of uncertainty in critical N concentration [%N<sub>c</sub>]. This study implements a partially-pooled Bayesian hierarchical method to develop CNDCs for previously published and newly reported experimental data, systematically evaluates the difference in %N<sub>c</sub> across  $G \times E \times M$  effects, and directly compare CNDCs from the Bayesian framework to CNDCs from conventional statistical methods. The partially-pooled Bayesian hierarchical method implemented in this study has the advantage of being less susceptible to inferential bias at the level of individual  $G \times E \times M$  interactions compared to alternative statistical methods which result from insufficient quantity and quality of experimental datasets (e.g., unbalanced distribution of N limiting and non-N limiting observations). This method also allows for a direct statistical comparison of differences in %N<sub>c</sub> [ $\Delta\%N_c$ ] across levels of the  $G \times E \times M$  interactions. Where found to be significant,  $\Delta\%N_c$  was attributed to variation in the timing of tuber initiation (e.g., maturity class) and the relative rate of tuber bulking (e.g., planting density) across  $G \times E \times M$  interactions. In addition to using the median value for %N<sub>c</sub> (i.e., CNDC), the boundary values for the credible region (i.e., CNDC<sub>lo</sub> and CNDC<sub>up</sub>) derived using the Bayesian framework should be used in calculation of N nutrition index (and other calculations) to account for and propagate uncertainty. Overall, this study provides additional evidence that %N<sub>c</sub> is dependent upon  $G \times E \times M$  interactions; therefore, evaluation of crop N status or N use efficiency must account for variation in %N<sub>c</sub> across  $G \times E \times M$  interactions.

**Keywords:** critical nitrogen dilution curve; nitrogen nutrition index; nitrogen use efficiency; potato; Bayesian; genotype-by-environment-by-management interactions

**Abbreviations:** NUE, nitrogen use efficiency; NUpE, nitrogen uptake efficiency; NUtE, nitrogen utilization efficiency; NNI, nitrogen nutrition index; CNDC, critical nitrogen dilution curve; CNUC, critical nitrogen uptake curve; CNUtEC, critical nitrogen utilization efficiency curve; W, total dry weight plant biomass;  $N_{\text{Plant}}$ , plant nitrogen content,  $\%N_{\text{Plant}}$ , plant nitrogen concentration;  $\%N_c$ , critical plant nitrogen concentration; NUtE<sub>c</sub>, critical nitrogen utilization efficiency;  $\Delta\%N_c$ , difference in critical nitrogen concentration;  $\%N_{c,\text{up}}$ , upper bounds of credible interval for critical nitrogen concentration;  $\%N_{c,\text{lo}}$ , lower bounds of credible interval for critical nitrogen concentration; NNI<sub>up</sub>, upper bound of credible interval for nitrogen nutrition index value; NNI<sub>lo</sub>, lower bound of credible interval for nitrogen nutrition index value; CNDC<sub>lo</sub>, lower boundary of credible region for critical nitrogen dilution curve; CNDC<sub>up</sub>, upper boundary of credible region for critical nitrogen dilution curve; G, genotype; E, environment; M, management; EONR, economically optimum nitrogen rate

## 1. Introduction

Identifying optimal crop nitrogen [N] status to maximize growth and yield production is an elusive goal. Traditionally, either the yield-goal approach or rate-response curves have been used to identify optimal N fertilizer application rate (Morris et al., 2018). The N nutrition index [NNI] is an alternative approach to the current paradigm and comprises a well-developed framework to determine optimal crop N status (Lemaire et al., 2019). Typically, NNI is used to determine crop N status using whole plant analysis and to direct adaptive N management within a growing season (Houlès et al., 2007; Morier et al., 2015). Unlike the yield-goal or rate-response approach where the optimal N fertilizer rate is empirically based on the marginal economic returns to yield from N fertilizer (i.e., economic optimum N rate [EONR]) under a given set of genotype [G], environment [E], and management [M] factors (Morris et al., 2018; Nigon et al., 2019), the NNI framework has conventionally been considered generalizable across  $E \times M$  effects (e.g., year-to-year, geographic, or cultural practices variability) and can be defined for any particular G effect (e.g., crop species or cultivar). In this manner, NNI is considered to represent intrinsic physiological properties (Sadras & Lemaire, 2014) rather than a parameter otherwise subject to variation under environmental conditions (e.g., net soil N supply) or management practices (e.g., rate, source, timing, and placement of N fertilizer).

The NNI approach is defined based on the allometric relationship of declining plant N concentration [%N<sub>Plant</sub>] with increasing plant biomass, referred to as the critical N dilution curve [CNDC], which defines the critical N concentration [%N<sub>c</sub>] below which relative growth rate is reduced (Gastal et al., 2015):

$$\%N_c = a W^{-b} \quad [1]$$

where  $W$  represents dry weight plant biomass, and  $a$  and  $b$  are empirically fitted parameters.

Parameter  $a$  is numerically equivalent to  $\%N_c$  expressed in units of  $\text{g N } 100 \text{ g}^{-1}$  when  $W$  is equal

to  $1 \text{ Mg ha}^{-1}$ , and parameter  $b$  effectively represents the rate of decline in  $\%N_c$  as  $W$  increases.

Using the CNDC, NNI values are then calculated as ratio of  $\%N_{\text{Plant}}$  and  $\%N_c$ :

$$\text{NNI} = \%N_{\text{Plant}} / \%N_c \quad [2]$$

When NNI is greater than 1.0, crop N status is said to be in excess, and crop growth is not limited

by N, while when NNI is less than 1.0, crop N status is deficient, and crop growth is limited by N.

At NNI equal to 1.0, crop N status is optimal (Lemaire & Gastal, 1997).

A robust theoretical framework has been developed to explain decline in N concentration as

biomass increases, but the application of this theory is most commonly restricted to the vegetative

period where only metabolic and structural tissues are present (Greenwood et al., 1990; Justes et

al., 1994; Sadras & Lemaire, 2014). Dilution of N in vegetative tissue occurs in relationship to an

increasing proportion of structural biomass, with low N concentration, relative to metabolic (i.e.,

photosynthetic) biomass, with high N concentration (Lemaire & Gastal, 1997; Gastal et al., 2015).

Multiple previous studies have extended and empirically validated the CNDC relationships beyond

its typical applications to describe declining N concentration over the entire crop growth cycle,

including periods of reproductive growth, by including consideration of storage tissues in addition

to structural and metabolic tissues (Greenwood et al., 1986; Duchenne et al., 1997; Plénet &

Lemaire, 2000; Herrmann & Taube, 2004). Dilution of N beyond the vegetative period primarily

occurs as low N biomass (i.e., starch) accumulates in storage tissues such as grain or tubers, and

the rate of decline is determined by the relative N concentration in storage biomass compared to

vegetative biomass (Duchenne et al., 1997; Plénet & Lemaire, 2000). Duchenne et al. (1997)



observed that as an increasing proportion of biomass accumulates in tubers, the rate of decline in N concentration increases with increasing biomass. Certain crops, such as potato, exclusively use a CNDC based on whole plant biomass due to the complex relationship between vine growth and tuber production (Duchenne et al., 1997; Bélanger et al., 2001a; Giletto & Echeverría, 2015; Ben Abdallah et al., 2016). Despite the validity of this approach, interpreting variation in CNDC observed between cultivars and geographies has been challenging.

However, recent work by Giletto et al. (2020) identified a mechanistic relationship underpinning the observed empirical relationships in N dilution for potato. The CNDC based on whole plant biomass reflects dilution in both the tuber and vine biomass, individually, and the increasing proportion of biomass allocated to low concentrations of N in biomass (i.e., tubers) as whole plant biomass increases. Giletto et al. (2020) also observed that varieties and locations with a greater proportion of biomass allocated to tubers have a greater value for parameter  $b$  of the CNDC, where parameter  $b$  of the CNDC represents the relative rate of decline in  $\%N_c$  as biomass increases.

Based on this framework developed by Giletto et al. (2020), it is reasonable to expect that variation in CNDC for potato would occur due to variation in total biomass and harvest index (i.e., timing of tuber initiation, relative rate of tuber bulking) across  $G \times E \times M$  gradients. Understanding the effects of  $G \times E \times M$  interactions on crop N requirements and status is critical to improving agronomic outcomes and N use efficiency [NUE] within cropping systems (Lemaire & Ciampitti, 2020).

Previous development of CNDCs for potato (Duchenne et al., 1997; Bélanger et al., 2001a; Giletto & Echeverría, 2015; Ben Abdallah et al., 2016) has been conducted using a non-uniform set of statistical methods and with limited quantification of uncertainty in either the range of plausible

1  
2  
3  
4 118 %N<sub>c</sub> values or the fitted parameter values themselves. This makes it difficult to ascertain whether  
5  
6 119 observed differences in CNDCs result from underlying  $G \times E \times M$  effects, are confounded by the  
7  
8  
9 120 limitations of the statistical approach, or biased due to insufficient quantity or quality of  
10  
11  
12 121 experimental data (e.g., unbalanced distribution of N limiting and non-N limiting observations).  
13  
14

15 122 The conventional approach to fit a CNDC consists of a two-step process: first, the critical points  
16  
17 123 from the relationship of %N<sub>Plant</sub> as a function of biomass are selected using statistical criteria;  
18  
19  
20 124 second, a negative exponential curve is fit to the subset of critical points using non-linear  
21  
22 125 regression. There are two commonly used statistical approaches to identify critical points: (1)  
23  
24  
25 126 linear-plateau curve fit and (2) ANOVA and protected multiple comparison.  
26  
27

28 127 Using a linear-plateau curve to derive critical points was originally suggested by Justes et al.  
29  
30  
31 128 (1994). This approach is rigorous and requires sufficient empirical data such that a linear-plateau  
32  
33 129 curve can be identified (i.e., at least one N limiting and at least two non-N limiting data points) for  
34  
35  
36 130 each observation date. Therefore, this approach can be difficult or impossible to implement due to  
37  
38 131 potential limitations of the experimental data used such as insufficient levels of N treatments (i.e.,  
39  
40  
41 132 fewer than three treatment levels) or interactions between management practices and  
42  
43 133 environmental conditions (i.e., all observations are either N limiting or non-N limiting).  
44  
45

46 134 In contrast, many studies use methods similar to Ben Abdallah et al. (2016) where critical points  
47  
48  
49 135 are determined using a simplified statistical method. In this approach, ANOVA is first used to  
50  
51 136 identify experimental dates where variation in biomass is statistically significant. Subsequently, a  
52  
53  
54 137 protected multiple comparisons analysis is used to identify which experimental treatments had the  
55  
56 138 highest level of biomass – the treatment level with the significantly greatest level of biomass is  
57  
58  
59 139 then defined as the critical point. While this statistical method is more flexible to implement, it  
60  
61  
62  
63  
64  
65

cannot resolve deficiencies in the underlying empirical data (e.g., insufficient level of N treatments, interactions with environmental conditions) that the linear-plateau method was designed to discriminate against. Therefore, the critical points selected using the simplified method may be biased due to inherent deficiencies of the underlying experimental data used.

Novel statistical methods developed first by Makowski et al. (2020) provide a framework which allows for standardization in statistical approach and quantification of uncertainty for deriving in CNDCs which enables direct comparison of %N<sub>c</sub> across  $G \times E \times M$  interactions. In short, this framework implements a hierarchical Bayesian model which simultaneously identifies critical points using the linear-plateau method (e.g., Justes et al. (1994)) while fitting the negative exponential curve which defines %N<sub>c</sub>. The advantage of this method is that it fits the CNDC from the entire set of experimental data for a given  $G \times E \times M$  interaction level and removes the arbitrary intermediate step of separately identifying critical points. This approach has already been successfully used by Ciampitti et al. (2021), Yao et al. (2021), and Fernández et al. (2021) to evaluate differences in CNDCs across  $G \times E \times M$  interactions for maize, wheat, and tall fescue cropping systems, respectively. Through this single-step process, the Bayesian hierarchical method both eliminates the need to separately identify critical points and implements the theoretically preferred method (e.g., linear-plateau curve fit) to select critical points.

However, the Bayesian hierarchical method remains subject to inferential bias due to both limited quantity and quality of experimental data (Fernández et al., 2021). With respect to quantity, having an insufficient number of observations from a limited number of experimental trials to derive an individual CNDC will result in increased bias in %N<sub>c</sub>. With respect to quality, using experimental data that does not reflect a full range of biomass values or does not sufficiently represent both limiting and non-limiting N conditions will result in increased bias in %N<sub>c</sub>. However, the approach

of fully pooling experimental data across  $G \times E \times M$  interactions may result in reduced inferential bias from the Bayesian hierarchical method by increasing the combined quantity and quality of data used to fit a given CNDC (Fernández et al., 2021).

Partial pooling, however, is an alternative statistical approach that may both reduce bias in  $\%N_c$  due to experimental data limitations and enable identifying individual CNDC for each given  $G \times E \times M$  interaction level. Balancing the tradeoffs between fitting a single population-level model (i.e., fully pooled) and fitting multiple independent group-level models (i.e., not pooled), the partial pooling approach uses the entire set of experimental data to fit a single model with where the data from all other levels of an effect influence the inference for a particular level and reduce inferential bias (McElreath, 2020). In this manner, individual effect levels are said to be “borrowing strength” through the process of “shrinkage”, where more extreme values are pulled toward the average (Lindstrom & Bates, 1990; Bates, 2010). Therefore, using a partially-pooled Bayesian hierarchical method should reduce the inferential bias for a given  $G \times E \times M$  interaction level where the quantity and quality of experimental data are not otherwise sufficient.

Building upon previous work, the objectives of this study are to 1) develop CNDCs using the hierarchical Bayesian framework for potato varieties in Minnesota (from both previously published and unpublished experimental data) and for potato varieties in Argentina (Giletto & Echeverría, 2015), Canada (Bélanger et al., 2001a), and Belgium (Ben Abdallah et al., 2016) (from previously published experimental data), 2) extend the implementation of the hierarchical Bayesian framework using a partial pooling approach to compare CNDCs across  $G \times E \times M$  interactions based on the uncertainty in  $\%N_c$  and curve parameters  $a$  and  $b$ , 3) identify the optimal methods to determine uncertainty in  $\%N_c$  for use in calculating NNI and other derivative metrics,

and 4) compare CNDCs developed with the hierarchical Bayesian framework methods to previously published CNDCs for the same data with different statistical methods.

## 2. Materials and Methods

### 2.1. Experimental Data

This study combines experimental data from both newly reported and previously published sources (Ben Abdallah et al., 2016; Giletto et al., 2020). The data used for analysis in this study are summarized in Table 1 and the relevant methods related to the experimental trials are reported below. All individual experimental observations used in this study are presented in the Supplemental Materials (Table S1).

**Table 1.** Summary of experimental data used in this study.

Study	Location	Variety	Site-Years	Sampling Dates	Samples
Present Study	Minnesota	Clearwater	2	10	30
		Dakota Russet	2	14	70
		Easton	2	14	70
		Russet Burbank	9	52	328
		Umatilla Russet	2	10	30
Giletto et al. (2020)	Argentina	Bannock Russet	3	13	52
		Gem Russet	4	18	72
		Innovator	4	18	72
		Markies Russet	2	9	36
		Umatilla Russet	3	14	56
	Canada	Russet Burbank	4	30	104
		Shepody	4	30	105
Ben Abdallah et al. (2016)	Belgium	Bintje	17	49	238
		Charlotte	7	24	114

#### 2.1.1. Newly Reported Data – Minnesota

Six individual plot-scale field experiments were conducted over a total of eight years (MN-1: 1991–1992; MN-2: 2014-2015, MN-3: 2016, MN-4: 2018-2019, MN-5: 2019, MN-6: 2020) on

irrigated plots at the Sand Plain Research Farm [SPRF] in Becker, MN (45° 23' N, 93° 53' W) (Table 2). The soil is characterized as a Hubbard loamy sand (Sandy, mixed, frigid Entic Hapludolls) with organic matter content ranging from 1.3 to 2.5% and is excessively well drained with low available water holding capacity (Hansen & Giencke, 1988; USDA NRCS, 2013). For a typical growing season beginning on 1 May and ending on 15 September, mean temperature is 18.9°C, cumulative precipitation is 383 mm, cumulative growing degree days are 1638 °C days, mean daily solar radiation is 22.7 MJ m<sup>-2</sup>, and mean diurnal temperature difference is 11.6 °C based on a historical climate reconstruction for the period of 1980-2016 (Gelaro et al., 2017; Weather Spark, 2021).

**Table 2.** Summary of newly reported experimental small-plot trials in Minnesota, USA.

Experiment	Year	Reference
MN-1	1991-1992	Rosen et al. (1992); Rosen et al. (1993); Errebhi et al. (1998)
MN-2	2014-2015	Sun (2017); Sun et al. (2019); Sun et al. (2020)
MN-3	2016	Crants et al. (2017)
MN-4	2018-2019	Gupta and Rosen (2019); Gupta et al. (2020); Li et al. (2021)
MN-5	2019	Bohman et al. (2020)
MN-6	2020	Rosen et al. (2021)

Apart from experimental N and variety treatments, all management and cultural practices were managed by the staff at the SPRF in accordance with common practices for the region (Egel, 2017). Nutrients were applied based on soil samples and University recommendations (Franzen et al., 2018; Rosen, 2018), and supplemental irrigation was applied based on the University recommended checkbook method (Wright, 2002; Steele et al., 2010). Additional details on experimental procedures for these studies have been previously reported (Table 2).

A randomized complete block design with three or four replicates was used in each field experiment. All studies evaluated at least 3 nitrogen rates (0 – 400 kg N ha<sup>-1</sup>) for Russet Burbank potato [*Solanum tuberosum* (L.)], with some studies evaluating additional potato varieties (Table 2). Nitrogen fertilizer was applied using various source and timing regimes including polymer coated urea applied at planting and/or emergence, split-applied urea and urea-ammonium nitrate at emergence and/or post-emergence, ammonium nitrate at planting, emergence, and/or post-emergence. The maturity class of varieties evaluated in these experiments included: medium-late – Clearwater and Dakota Russet; medium-late to late – Umatilla Russet; late – Easton; late to very late – Russet Burbank (Thompson, 2013; Porter, 2014; Stark et al., 2020; OSU, 2021). Planting density was 36,000 plants ha<sup>-1</sup> for all experiments except for MN-1 which was planted at a density of 48,000 plants ha<sup>-1</sup>.

The experiments that evaluated multiple varieties had either a factorial design, or split-plot design with variety treatment as the whole-plot and nitrogen treatment as the split-plot. Plots in these studies were between 5.4 – 6.4 m wide (6 or 7 x 0.9 m rows) and 6.1 – 9.1 m long. Experiments were planted each year in late-April to early-May and were mechanically harvested in mid-September with vines terminated one to two weeks prior to harvest. A summary of N management practices and varieties evaluated for each of these studies is given below (Table 3).

**Table 3.** Summary of experimental treatments evaluated in small-plot trials in Minnesota, USA.

Experiment	N treatments <sup>†</sup>	N rates	Varieties
MN-1	10	0, 135, 180, 225, 270	Russet Burbank
MN-2	5	135, 200, 270, 335, 400	Russet Burbank, Dakota Russet, Easton
MN-3	4	45, 180, 245, 335	Russet Burbank
MN-4	3	135, 270, 400	Russet Burbank, Clearwater, Umatilla Russet
MN-5	8	45, 155, 245, 290, 335	Russet Burbank
MN-6	8	55, 155, 245, 270, 290, 335	Russet Burbank

<sup>†</sup> Including N source, timing, and placement combinations occurring at an equivalent N rate

Samples of vine biomass were harvested immediately prior to mechanical termination for determination of fresh weight vine yield. Harvested tubers were mechanically sorted into weight classes and graded (USDA, 1997), and fresh weight tuber yield was determined as the sum of all weight classes and tuber grades. Harvested biomass was oven dried at 60°C to determine dry matter content of vines and tubers. Dry weight tuber and vine biomass was calculated as the product of fresh weight and dry matter content for each tissue respectively. Total N concentration of vines and tubers was determined from subsamples of plant tissues with either combustion analysis (Elementar Vario EL III, Elementar Americas Inc., Mt. Laurel, NJ) using standard methods (Horneck & Miller, 1998), or with the salicylic Kjeldahl method (Horwitz et al., 1970). Total N content of vines and tubers was calculated as the product of N concentration and dry weight biomass for each tissue respectively. Total plant N content [ $N_{\text{Plant}}$ ] ( $\text{kg N ha}^{-1}$ ) was calculated from the sum of tuber and vine N content. Total plant dry weight biomass [ $W$ ] ( $\text{Mg dry wt. ha}^{-1}$ ) was calculated from the sum of vine and tuber dry weight biomass. Plant N concentration [% $N_{\text{Plant}}$ ] ( $\text{g N } 100 \text{ g}^{-1} \text{ dry wt.}$ ) was calculated as the ratio of  $N_{\text{Plant}}$  to  $W$ .



Whole-plant samples were also regularly collected during the period of late-May to early-September (Table 4). Two to three plants were harvested from each plot on four to six dates each year with vines, roots, and tubers each measured separately. Dry weight biomass, N concentration, and N content for vines and tubers were determined for these in-season plant tissue samples using the methods described above. Calculations for  $W$ ,  $N_{\text{Plant}}$ , and  $\%N_{\text{Plant}}$  were the same as methods previously described above.

**Table 4.** In-season and harvest sampling dates for the experimental small-plot trials in Minnesota, USA.

Experiment	Year	In-Season						Harvest
		1	2	3	4	5	6	
MN-1	1991	12 June	24 June	2 July	16 July	30 July	13 Aug	10 Sept.
MN-1	1992	10 June	25 June	17 July	5 Aug.	26 Aug.		15 Sept.
MN-2	2014	30 June	15 July	24 July	11 Aug.	26 Aug.	8 Sept.	15 Sept.
MN-2	2015	23 June	7 July	21 July	4 Aug.	17 Aug.	1 Sept.	16 Sept.
MN-3	2016	28 June	13 July	26 July	3 Aug.	10 Aug.		13 Sept.
MN-4	2018	26 June	10 July	18 July	1 Aug.			13 Sept.
MN-4	2019	26 June	11 July	24 July	7 Aug			16 Sept.
MN-5	2019	25 June	9 July	23 July	6 Aug	21 Aug		16 Sept.
MN-6	2020	24 June	7 July	22 July	4 Aug			16 Sept.

#### 2.1.2. Previously Published Data – Belgium, Argentina, and Canada

Experimental data reported in two previous studies, Giletto et al. (2020) and Ben Abdallah et al. (2016), were included in the analysis conducted for the present study. The data from Giletto et al. (2020) comprises two separate experimental data sets from Argentina (Giletto & Echeverría, 2015) and Canada (Bélanger et al., 2000, 2001a, 2001b). All data from the Giletto et al. (2020) study used in the present analysis was included in this previous publication.

In the Canadian study, two varieties (Russet Burbank and Shepody) and four N fertilization rates (0, 50, 100, and 250 kg ha<sup>-1</sup>) were evaluated under irrigated and non-water limiting conditions with

each variety having four site-years of experimental data and either seven or eight sampling dates per site-year (Table 1). These small-plot experiments were conducted in the upper St. John River Valley of New Brunswick, Canada (47° 03' N; 67° 45' W). Nitrogen fertilizer for all treatments was ammonium nitrate applied at planting. The maturity class of varieties evaluated in these experiments included: early to medium-early – Shepody; late to very late – Russet Burbank (Stark et al., 2020; OSU, 2021). Planting density was 29,000 and 44,000 plants ha<sup>-1</sup> for Russet Burbank and Shepody, respectively. The soil texture for these experiments was classified as either loam or clay loam with organic matter content ranging from 2.6 to 3.0%. For a typical growing season beginning on 1 June and ending on 10 October, mean temperature is 15.7°C, cumulative precipitation is 371 mm, cumulative growing degree days are 1150 °C days, mean daily solar radiation is 19.1 MJ m<sup>-2</sup>, and mean diurnal temperature difference is 10.0 °C based on a historical climate reconstruction for the period of 1980-2016 (Gelaro et al., 2017; Weather Spark, 2021).

In the Argentina study, five varieties (Bannock Russet, Gem Russet, Innovator, Markies Russet, and Umatilla Russet) and four N fertilization rate (0, 80, 150, and 250 kg N ha<sup>-1</sup>) were each evaluated under irrigated and non-water limiting conditions for between two and four site-years with between four and five sampling dates per site year (Table 1). These small-plot experiments were conducted in Balcarce in the province of Buenos Aires, Argentina (37° 45' S; 58° 18' W). Nitrogen fertilizer for all treatments was urea applied at planting. The maturity class of varieties evaluated in these experiments included: early to medium – Innovator; medium to late – Gem Russet; medium-late to late – Umatilla Russet; late to very late – Bannock Russet and Markies Russet (Giletto & Echeverría, 2015; Stark et al., 2020; OSU, 2021). The planting density was 59,000 plants ha<sup>-1</sup> for all varieties. The soil texture for these experiments was classified as loam with organic matter content ranging from 4.2 to 5.2%. For a typical growing season beginning on

1  
2  
3  
4 287 10 October and ending on 10 March, mean temperature is 18.4°C, cumulative precipitation is 428  
5  
6 288 mm, cumulative growing degree days are 1739 °C days, mean daily solar radiation is 25.5 MJ m<sup>-2</sup>,  
7  
8  
9 289 <sup>2</sup>, and mean diurnal temperature difference is 13.6 °C based on a historical climate reconstruction  
10  
11  
12 290 for the period of 1980-2016 (Gelaro et al., 2017; Weather Spark, 2021).

13  
14  
15 291 The data from Ben Abdallah et al. (2016) represents multiple experimental data set from Belgium.  
16  
17 292 Only a portion of the data from the Ben Abdallah et al. (2016) study used in the present analysis  
18  
19  
20 293 was included in this previous publication – while the dry weight biomass data were previously  
21  
22 294 reported, the N concentration data from the Ben Abdallah et al. (2016) experiment is reported for  
23  
24  
25 295 the first time in this work.

26  
27  
28 296 In the Belgium studies, three to six N rates (ranging from 0 to 250 kg N ha<sup>-1</sup>) were evaluated for  
29  
30  
31 297 two varieties (Bintje and Charlotte) for 17 and 7 site-years, respectively, with between one and  
32  
33 298 eight sampling dates per site year (Table 1). These small-plot experiments were conducted in  
34  
35 299 Gembloux, Belgium (50° 33' N; 4° 43' E). Nitrogen fertilizer for all treatments was ammonium  
36  
37  
38 300 nitrate applied at planting. The maturity class of varieties evaluated in these experiments included:  
39  
40 301 medium – Charlotte; late – Bintje (CFIA, 2013; AHDB, 2015; OSU, 2021). The planting density  
41  
42  
43 302 was 38,000 plants ha<sup>-1</sup> for all varieties. The soil texture for these experiments was classified as  
44  
45 303 loam, sandy loam, silt loam, or silty clay loam with organic matter content ranging from 1.3 to  
46  
47  
48 304 2.6%. For a typical growing season beginning on 20 April and ending on 20 September, mean  
49  
50 305 temperature is 15.5°C, cumulative precipitation is 244 mm, cumulative growing degree days are  
51  
52 306 1313 °C days, mean daily solar radiation is 20.0 MJ m<sup>-2</sup>, and mean diurnal temperature difference  
53  
54  
55 307 is 8.3 °C based on a historical climate reconstruction for the period of 1980-2016 (Gelaro et al.,  
56  
57 308 2017; Weather Spark, 2021).

1  
2  
3  
4  
5  
6  
7  
8  
9  
10  
11  
12  
13  
14  
15  
16  
17  
18  
19  
20  
21  
22  
23  
24  
25  
26  
27  
28  
29  
30  
31  
32  
33  
34  
35  
36  
37  
38  
39  
40  
41  
42  
43  
44  
45  
46  
47  
48  
49  
50  
51  
52  
53  
54  
55  
56  
57  
58  
59  
60  
61  
62  
63  
64  
65

309 A comparison of G (i.e., maturity class), E (i.e., soil texture, growing season weather conditions),  
310 and M (i.e., planting density, source and timing of N fertilizer) factors across the  $G \times E \times M$   
311 interaction levels evaluated in this study is presented in Table 5.

312

**Table 5.** Comparison of key experimental factors including for Genotype [G]: variety maturity class [Maturity Class]; Environment [E]: soil texture classification [Soil Texture], soil organic matter content [OM], growing season mean daily temperature [ $T_{\text{Mean}}$ ], growing season cumulative precipitation [Precip.], growing season mean diurnal temperature difference [ $\Delta T_{\text{Diurnal}}$ ], growing season cumulative growing degree days [GDD], growing season mean daily incident solar radiation [Sol. Rad.]; and Management [M]: planting density [Density], and N fertilizer application source and timing.

		<b>G</b>	<b>E</b>							<b>M</b>	
Location	Variety	Maturity Class <sup>†</sup>	Soil Texture <sup>‡</sup>	OM [%]	$T_{\text{Mean}}$ [°C]	Precip. [mm]	$\Delta T_{\text{Diurnal}}$ [°C]	GDD [°C d]	Sol. Rad. [MJ m <sup>-2</sup> ]	Density [plants ha <sup>-1</sup> ]	N Source & Timing <sup>§</sup>
Argentina	Bannock Russet	L to VL	L	4.2 to 5.2	18.4	428	13.6	1739	25.5	59,000	Urea @ PL
	Gem Russet	M to L									
	Innovator	E to M									
	Markies Russet	L to VL									
	Umatilla Russet	ML to L									
Belgium	Bintje	L	SiCL, SiL, L, SL	1.3 to 2.6	15.5	244	8.3	1313	20.0	38,000	AN @ PL
	Charlotte	M									
Canada	Russet Burbank	L to VL	CL, L	2.6 to 3.0	15.7	371	10.0	1150	19.1	29,000	AN @ PL
	Shepody	E to ME								44,000	
Minnesota	Clearwater	ML	LS	1.3 to 2.5	18.9	383	11.6	1638	22.7	36,000	AN, Urea, UAN, and/or PCU @ PL, EM, and/or P-EM
	Dakota Russet	ML									
	Easton	L									
	Russet Burbank	L to VL									
	Umatilla Russet	ML to L									

<sup>†</sup> Early [E], medium-early [ME], medium [M], medium-late [ML], late [L], very late [VL]

<sup>‡</sup> Silty clay loam [SiCL], clay loam [CL], silt loam [SiL], loam [L], sandy loam [SL], loamy sand [LS]

<sup>§</sup> Ammonium nitrate [AN], urea-ammonium nitrate [UAN], polymer-coated urea [PCU], planting [PL], emergence [EM], post-emergence [P-EM]

## 2.2. Statistical Methods

Based on the general approach outlined by Makowski et al. (2020), this study implemented a partially-pooled Bayesian hierarchical framework to infer CNDC parameters for each location and variety within location, assess the uncertainty in model parameters and %N<sub>c</sub>, and compare fitted CNDCs across the effects of location and variety.

In summary, this statistical approach uses the entire set of experimental data (Figure 1a) and does not require any preliminary or intermediary statistical analysis. At the level of each experimental sampling date, a linear-plateau curve is fit for biomass as a function of N concentration (Figure 1b) and the join point of the linear-plateau curve is used to define the %N<sub>c</sub>. Simultaneously, a negative exponential curve (i.e., CNDC) is fit across all experimental sampling dates for a given effect level of the hierarchical model (e.g., location, variety) where the critical point of each linear-plateau curve lies exactly upon the negative exponential curve (Figure 1b). In this manner, the linear-plateau curve fitted for any given date is influenced by the data from all other experimental sampling dates through the fitting of the negative exponential curve. In comparison, the conventional statistical approach fits a negative exponential curve to the subset of critical points (Figure 1c) which are identified via an intermediate statistical analysis (i.e., ANOVA and protected multiple comparisons).

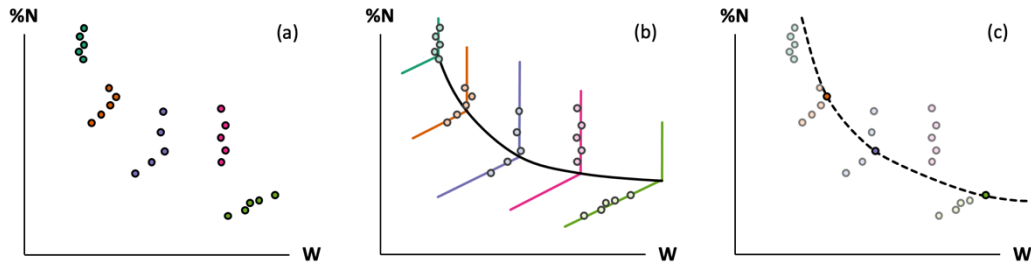


**Figure 1.** Hypothetical example comparing various statistical methods where plant N concentration [%N] as a function of biomass [W] on five experimental sampling dates for (a) raw experimental data, (b) linear-plateau curves (solid colored lines) fitted for each experimental sampling date (points for each date distinguished by color) and the critical N dilution curve (solid black line) fitted using the hierarchical Bayesian method based on Makowski et al. (2020), and (c) critical points (opaque) and non-critical points (transparent) selected using conventional statistical analysis (i.e., ANOVA and protected multiple comparison) with critical N dilution curve (dotted line) fitted using conventional methods (i.e., non-linear regression using only the critical points).

The Bayesian hierarchical framework outlined by Makowski et al. (2020) was extended to explicitly include  $G \times E \times M$  interaction levels within the fitted model using a partial pooling approach. Experimental data were nested according to location and variety within location, where the linear-plateau curve fitted for each experimental sampling date is nested within a given level of variety within location (Figure 2). This model structure leverages the advantages of partial pooling to addresses the limitations identified by Fernández et al. (2021) that a sufficient quantity and quality of experimental data are required while still enabling direct inference on the individual  $G \times E \times M$  interaction levels. Using *R* (R Core Team, 2021a), the *brms* package (Bürkner, 2017, 2018) was used to implement the statistical framework outlined by Makowski et al. (2020) with the modifications as previously described (Figure 2). The *brms* package, an interface to *Stan* (Carpenter et al., 2017), was chosen due to the ability to include group-level (i.e., random effects) which allows for the fit of this particular partially-pooled Bayesian hierarchical model. The *brms* package includes a user-friendly modeling language, robust documentation, and a diverse set of tools to analyze and assess models.

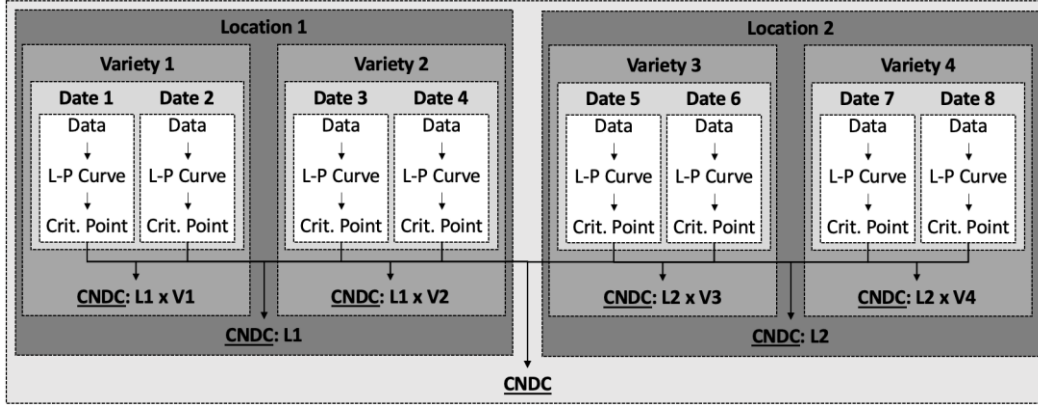


**Figure 2.** Flowchart showing nested structure used to fit critical N dilution curves [CNDC] using the hierarchical Bayesian method based on Makowski et al. (2020). Linear-plateau (L-P) curves and critical points (i.e., the fitted join point of each linear-plateau curve) are identified at the level of each experimental sampling date and pooled at various levels of location and variety within location to determine the CNDC for that level. This hierarchical model structure simultaneously fits all individual levels of location and variety within location, as well as for the global level of all experimental data, which allows for direct comparison across levels.

A non-linear *brms* model was defined by combining the two separate expressions used by Makowski et al. (2020) to parameterize the Bayesian hierarchical model as previously implemented with *rjags* (Plummer, 2019) and *JAGS* statistical software (Plummer, 2013).

The first expression from Makowski et al. (2020) represents the linear-plateau component:

$$W = \min(W_{Max,i} + S_i \cdot (\%N_{Plant} - \%N_c), W_{Max,i}) \quad [3]$$

where  $S_i$  and  $W_{Max,i}$  are the slope of the linear-plateau curve and the maximum value of biomass (i.e., plateau) for a given date [i], respectively, *min* represents the minima function (i.e., the plateau component), and  $W$ ,  $\%N_{Plant}$ , and  $\%N_c$  have the same meaning as previously defined in this present study. This linear-plateau curve is defined with N concentration as the independent variable and biomass as the dependent variable and is written in point-slope form where the reference point used is the critical point.

The second expression from Makowski et al. (2020) represents the CNDC component:



$$\%N_c = a W_{Max,i}^{-b} \quad [4]$$

where  $a$  and  $b$  are the parameters that define the negative exponential curve and  $\%N_c$  and  $W_{Max,i}$  have the same meanings as defined above.

Using algebraic substitution (i.e., for  $\%N_c$ ), these two expressions (Eq. [3] and Eq. [4]) were combined to produce following non-linear *brms* model formula:

$$W \sim \min(W_{Max,i} + S_i (\%N_{Plant} - (a W_{Max,i}^{-b})), W_{Max,i}) \quad [5]$$

Two group-level (i.e., random) effects were specified for this *brms* model to parameterize the nested structure (Figure 2). First, the parameters  $S$  and  $W_{Max}$  included group-level effects to fit a linear-plateau curve to each experimental sampling date:

$$W_{Max} + S \sim 1 + (1 | index) \quad [6]$$

where *index* represents the unique level of each experimental sampling date, nested within a given level of variety within location. Second, the parameters  $a$  and  $b$  included group-level effects to fit the CNDC:

$$a + b \sim 1 + (1 | location) + (1 | location:variety) \quad [7]$$

where *location* and *location:variety* represents the unique effect level for location and variety within location, respectively.

The *brms* model was fitted using 4 chains and 10000 iterations with 3000 warmups per chain. The priors for this model were chosen based on expert knowledge (i.e., previously reported values), empirical observations (i.e., summary values from the data set), and the joint prior predictive distribution (i.e., if a set of relatively uninformative priors led to biologically or physically

impossible predictions, the prior ranges were narrowed) (Schad et al., 2021). This is particularly important for hyperparameters dealing with the standard deviation between groups in a hierarchical model. A summary of the prior values used in this model is given below (Table 6).

**Table 6.** Priors used in fitting the hierarchical Bayesian model with brms.

Parameter	Distribution	Bounds	
		Lower	Upper
$a$	Normal (5.3, 0.1)	0	$\infty$
$\sigma(a_{location})$	Normal (0.10, 0.02)	$-\infty$	$\infty$
$\sigma(a_{location:variety})$	Normal (0.05, 0.01)	$-\infty$	$\infty$
$b$	Normal (0.40, 0.01)	0	1
$\sigma(b_{location})$	Normal (0.05, 0.02)	$-\infty$	$\infty$
$\sigma(b_{location:variety})$	Normal (0.02, 0.01)	$-\infty$	$\infty$
$W_{max}$	Normal (8.0, 0.1)	1	$\infty$
$\sigma(W_{max:index})$	Normal (7.0, 1.0)	$-\infty$	$\infty$
$S$	Normal (6.0, 0.1)	0	$\infty$
$\sigma(S_{index})$	Normal (1.0, 0.1)	$-\infty$	$\infty$
$\sigma$	Student's $t$ (3, 1.0, 0.1)	$-\infty$	$\infty$

The entire statistical and data workflow used to generate this analysis is reproducible and available via GitHub repository (<https://github.com/bohm0072/bayesian-cnndc-potato>). The *renv* package (Ushey, 2021) was used to document the computing environment utilized while conducting this analysis to ensure code portability and reproducibility.

## 2.3. Evaluating Uncertainty

### 2.3.1. Critical N Dilution Curve Parameter Uncertainty

After the statistical model was successfully fit to the data (n=28,000 draws), values for parameters  $a$  and  $b$  of the CNDC were reported at the 0.05, 0.50 (i.e., median) and 0.95 quantiles for the effect levels of *location* and *location:variety* to determine the 90% credible interval for each parameter. The correlation between values for parameters  $a$  and  $b$  was determined for each effect level of *location:variety* using the fitted parameter values at the level of the individual draws.

### 2.3.2. Critical N Concentration Uncertainty

The %N<sub>c</sub> for a set of discrete values of  $W$  between 1 Mg dry wt. ha<sup>-1</sup> and the maximum observed value of  $W$  in the experimental data set was calculated for each individual draw based on the fitted values of parameters  $a$  and  $b$  for that draw. From the distribution of %N<sub>c</sub> values, the 0.05, 0.50 (i.e., median) and 0.95 quantile values were identified for each effect level of *location:variety* to determine the 90% credible region for %N<sub>c</sub>. This approach makes maximal use of the jointly estimated parameters contained in the posterior distribution.

To develop curves approximating the upper and lower boundaries of the 90% credible region for %N<sub>c</sub> (i.e., the 0.05 and 0.95 quantile values, respectively), a negative exponential curve of the same form as the CNDC (i.e.,  $y = a x^{-b}$ ) was fit using *nls* (R Core Team, 2021b) to the set of data previously identified as defining the boundaries of the 90% credible region (i.e., 0.05 and 0.95 quantile values). These curves approximating the upper and lower boundaries of the credible region for the CNDC are respectively referred to as CNDC<sub>up</sub> and CNDC<sub>lo</sub>, where parameters  $a_{up}$  and  $b_{up}$  correspond to CNDC<sub>up</sub> and parameters  $a_{lo}$  and  $b_{lo}$  correspond to CNDC<sub>lo</sub>.

Additionally, an estimate of the 90% credible region was calculated by using the boundary values of the 90% credible interval of parameters  $a$  and  $b$ . The estimate for the upper boundary of the credible region for %N<sub>c</sub> was determined from the 0.95 quantile value for parameter  $a$  and 0.05 quantile value for parameter  $b$ ; the estimate for the lower boundary of the credible region of %N<sub>c</sub> was determined from the 0.05 quantile value for parameter  $a$  and 0.95 quantile value for parameter  $b$ . This approach does not account for the joint estimation of parameters offered by the Bayesian approach; therefore, the paired combination for parameters  $a$  and  $b$  (i.e., 0.05 and 0.95 quantiles) might not actually occur in the posterior distribution.

To compare the various methods described above, the difference in critical N concentration [ $\Delta\%N_c$ ] was calculated between the 0.50 quantile (i.e., median) value for  $\%N_c$ , designated as the reference values (i.e.,  $\Delta\%N_c$  with constant value of zero), and the various methods to quantify uncertainty (i.e., 90% credible region for  $\%N_c$ ,  $CNDC_{up}$  &  $CNDC_{lo}$ , and estimates of credible region for  $\%N_c$  using 90% credible interval for parameters  $a$  and  $b$ ). In this manner, the  $\Delta\%N_c$  for each method to quantify uncertainty in  $\%N_c$  can be directly compared.

### 2.3.3. Comparing Critical N Concentration across $G \times E \times M$ Effects

Similar to the above methods, the  $\%N_c$  for each draw was calculated across a set of discrete values of  $W$  over the range of 1 Mg dry wt.  $ha^{-1}$  and the maximum observed value of  $W$  in the experimental data set. At the effect level of *location:variety*, the difference between the  $\%N_c$  for a given comparison and reference  $CNDC$  (i.e.,  $\Delta\%N_c$ ) was calculated at each value of  $W$ . From this computed set of  $\Delta\%N_c$ , the 0.05, 0.50 (i.e., median) and 0.95 quantile values were identified for each effect level of *location:variety* to determine the 90% credible region for  $\Delta\%N_c$ . For a given range of  $W$  values, the comparison curve considered to be not significantly different from the reference curve if the  $\Delta\%N_c$  values for the 0.05 and 0.95 quantile values of  $\%N_c$  were respectively less than and greater than zero (i.e., the 90% credible region for  $\Delta\%N_c$  contains zero). In the case where the 0.05 quantile value for  $\Delta\%N_c$  was greater than zero, the comparison curve was considered to have a significantly greater  $\%N_c$  than the reference curve. In the case where the 0.95 quantile value for  $\Delta\%N_c$  was less than zero, the comparison curve was considered to have a significantly lower  $\%N_c$  than the reference curve. To evaluate  $\Delta\%N_c$  in the present study, the  $\%N_c$  for a given effect level of *location:variety* was compared to all other levels, and this approach allows for the direct evaluation of  $\Delta\%N_c$  across  $G \times E \times M$  effects.

#### 2.3.4. Comparing Critical N Concentration across Statistical Methods

An analogous method was also used to compare the CNDCs fitted in the present study to the CNDCs published in previous studies (i.e., Ben Abdallah et al. (2016); Giletto et al. (2020)). Specifically, the previously published curves were evaluated to see if they fell within the 90% credible region for the corresponding curve fitted with the hierarchical Bayesian method in the present study. Using the determined credible region for  $\%N_c$ , it is possible to identify the range for which two CNDCs are significantly different. If the previously identified  $\%N_c$  value falls outside of the credible region for  $\%N_c$  identified in this study, then the two curves are determined to be significantly different over the range for which the previous value falls outside of the credible region. This approach allows for direct evaluation of differences in  $\%N_c$  for CNDCs developed from the same set of data across various statistical methods.

### 3. Results

#### 3.1. Fitted Critical N Dilution Curve

The posterior distribution of fitted values for CNDC parameters  $a$  and  $b$  are presented below (Figure 3) showing the median value and 90% credible interval (i.e., 0.05 and 0.95 quantile values). For parameter  $a$ , there was no significant difference for the effect of location at 90% credible interval threshold (Figure 3a). Although Argentina has a numerically greater value of parameter  $a$  (4.95) than the other three locations (4.74 – 4.77), these differences are not significant. Additionally, the variation in parameter  $a$  for the variety within location effect is negligible and not statistically significant (Figure 3a).

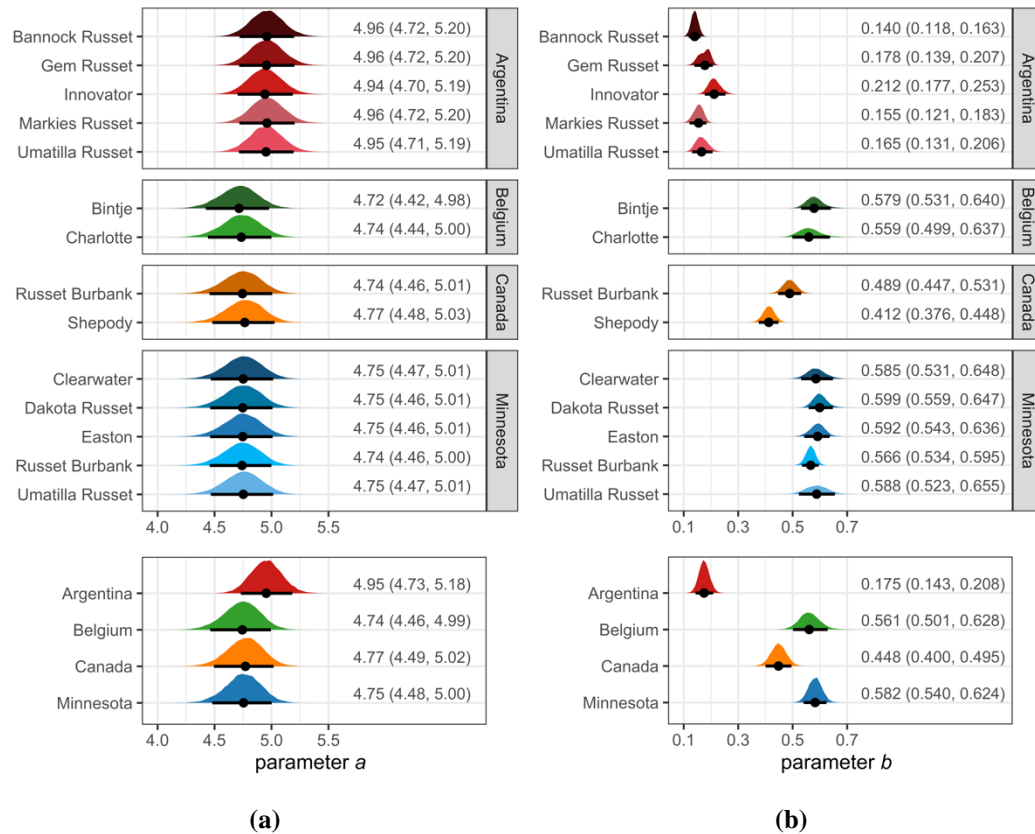


**Figure 1.** Posterior distribution of variety and variety within location effects for (a) parameter  $a$ ; and (b) parameter  $b$ . Points represent median value and line represents 0.05 and 0.95 quantile range. Values displayed with the figures are the median value with the 90% credible interval boundaries (i.e., 0.05 and 0.95 quantiles) displayed within the parentheses.

For parameter  $b$ , there were significant differences for both the effect of location and variety within location at a 90% credible interval threshold (Figure 3b). For location, Argentina had the lowest value for parameter  $b$  (0.175), while Canada had a greater value for parameter  $b$  (0.448) than Argentina but lower than either Belgium (0.561) or Minnesota (0.582). The difference between parameter  $b$  for Belgium and Minnesota was not significant. For the variety within location effect, parameter  $b$  significantly varied for varieties in Argentina and Canada, while there were no significant differences in parameter  $b$  within either Belgium or Minnesota. For Argentina, Innovator had the greatest value for parameter  $b$  (0.212), followed by Gem Russet, Umatilla Russet, Markies Russet, and Bannock Russet (0.178, 0.165, 0.155, and 0.140, respectively). The

difference between Innovator and Umatilla Russet, Markies Russet, and Bannock Russet was significant, while all other differences between varieties were not significant. For Canada, Russet Burbank had a significantly higher value for parameter  $b$  (0.489) than Shepody (0.412).

There was a positive correlation found between parameters  $a$  and  $b$  (Figure 4) which indicates that quantifying differences in these parameter values independently (Figure 3) is not appropriate to describe the uncertainty in %N<sub>c</sub> determined by the correlated parameters. Stated alternatively, significant differences for either parameter  $a$  or  $b$  do not necessarily imply that differences in %N<sub>c</sub> are also significant.

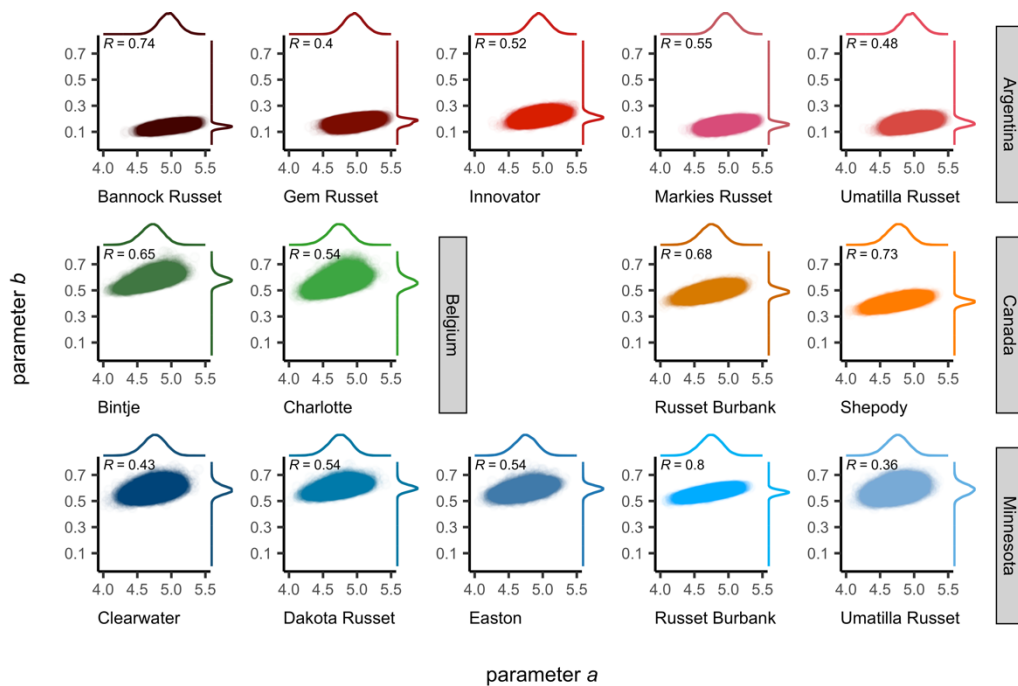


**Figure 2.** Distribution of posterior values for parameters  $a$  and  $b$  for each location within variety shown as a scatterplot with marginal density distribution given for each parameter. Pearson correlation coefficient  $[R]$  is displayed for the relationship between parameters  $a$  and  $b$ . Data are shown at the level of individual draws ( $n=28,000$ ).

Critical N dilution curves for each variety within location and the experimental data, median linear-plateau curve for each experimental sampling date, and median value of %N<sub>c</sub> are presented (Figure

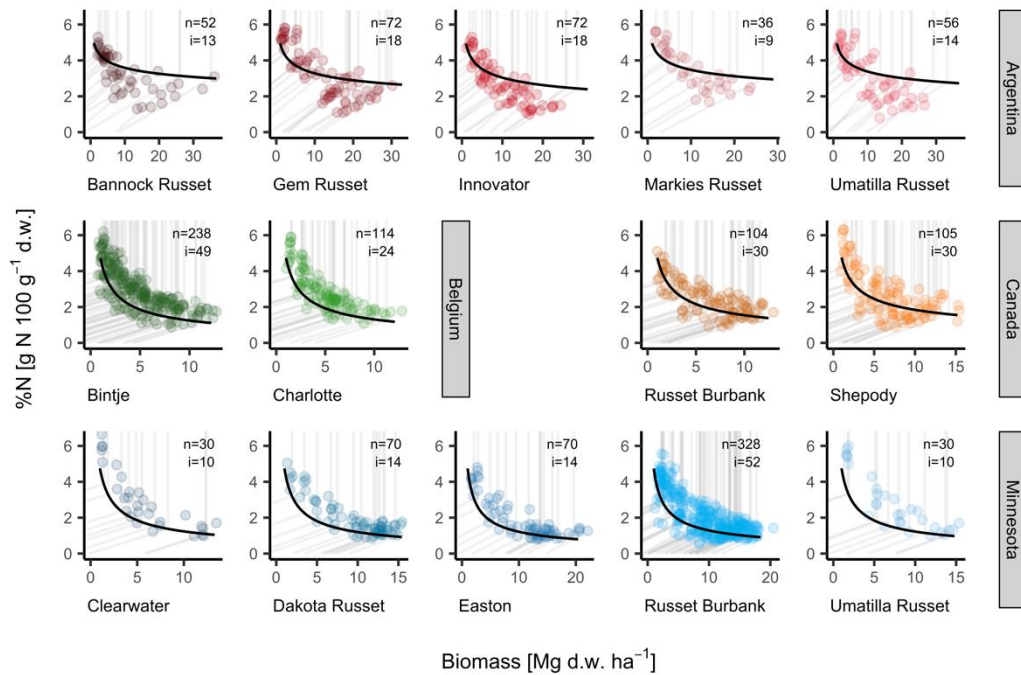


**Figure 3.** Critical N dilution curves (i.e., median value of critical N concentration [%N<sub>c</sub>]) fitted from the hierarchical Bayesian model are shown as a solid black lines for each location with variety. Biomass and N concentration [%N] data are displayed as points with the median linear-plateau curve for each sampling date shown as grey line. The number of samples [n] and the number of sampling dates [i] are displayed on each individual panel.

For the Argentina varieties, more than 60% of the observed data fall below the CNDC (i.e., represent N limiting conditions) with over 40% of sampling dates having exclusively N limiting conditions observed. For both the Belgium and Minnesota varieties, more than 80% of the observed data fall above the CNDC (i.e., represent non-N limiting conditions) with almost 30% of sampling dates having exclusively non-N limiting conditions observed. For the Canada varieties, over 60% of observed data represented non-N limiting conditions but less than 10% of sampling dates had exclusively non-N limiting conditions observed (Figure S1).



### 3.2. Critical N Concentration Uncertainty

The credible region for %N<sub>c</sub> varies across variety within location and across levels of biomass (Figure 6). The symmetry of the credible region distribution varies by variety within location. Some levels of variety within location, such as Argentina × Gem Russet, have a skewed distribution, while other levels, such as Canada × Shepody, have a symmetrical distribution (Figure 6a). There are also differences in the range of the credible region, where some varieties within location, such as Argentina × Umatilla Russet, have greater uncertainty in %N<sub>c</sub> than others, such as Minnesota × Russet Burbank. The uncertainty in %N<sub>c</sub> also varies across the level of biomass for a given CNDC. For example, as the level of biomass increases, Argentina × Umatilla Russet has an increasing credible region range, Minnesota × Russet Burbank has a decreasing credible region range, and Argentina × Bannock Russet has a nearly constant credible region range.

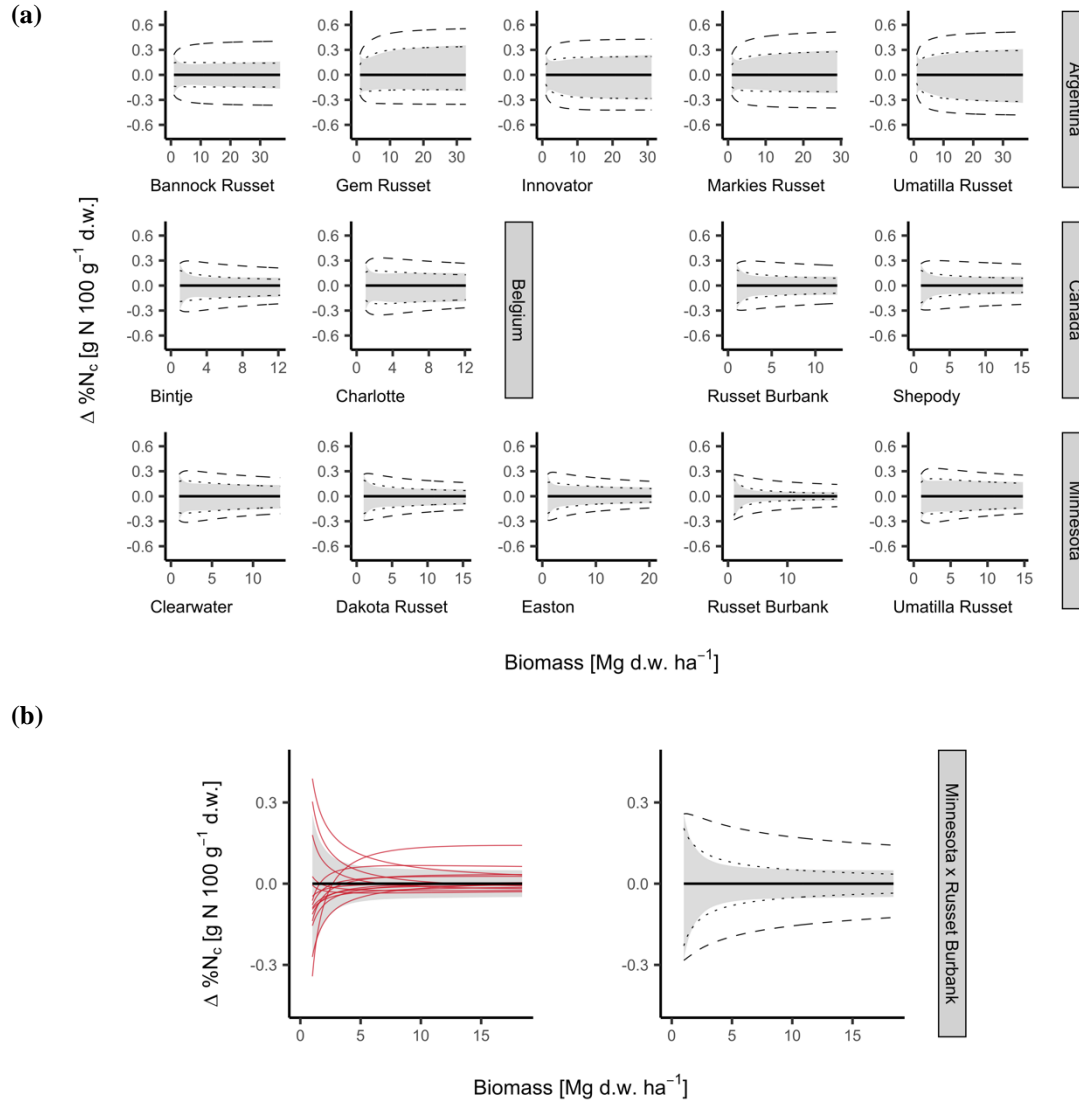


**Figure 4.** Comparison of the difference in critical N concentration values [ $\Delta\%N_c$ ] between the median critical N concentration, represented as a solid black line at constant  $\Delta\%N_c$  value of zero, and the various methods to quantify uncertainty in critical N concentration [ $\%N_c$ ] where the magnitude of uncertainty in  $\%N_c$  is equivalent the  $\Delta\%N_c$  value. The grey shaded region represents the 90% credible region (lower bound, 0.05 quantile; upper bound, 0.95 quantile) for the fitted Bayesian hierarchical model. The dotted lines represent an estimation of the upper and lower bound of the 90% credible region from using the non-linear regression method (i.e.,  $CNDC_{lo}$  and  $CNDC_{up}$ ). The dashed lines represent an approximation of uncertainty in  $\%N_c$  based on the posterior distribution of critical N dilution curve [CNDC] parameters  $a$  and  $b$ . Data are presented for (a) all levels of variety within location, and (b) shown in greater detail for Minnesota  $\times$  Russet Burbank only for individual draws from the Bayesian hierarchical model, for the non-linear regression method, and for the approximation of the 90% credible region based on the posterior distribution of parameters  $a$  and  $b$ . For (b), the solid red line represents individual draws ( $n=15$ ) from the posterior distribution of the fitted Bayesian hierarchical model.

Estimation of the upper and lower boundaries of the 90% credible region using the non-linear regression method (i.e.,  $CNDC_{lo}$  and  $CNDC_{up}$ ) (Table 7) appears to be reasonable based on graphical evaluation (Figure 6). However, these fitted  $CNDC_{lo}$  and  $CNDC_{up}$  curves do not themselves represent a draw directly from the posterior distribution and do not necessarily represent the most extreme possible curves (e.g., it is plausible to have an individual draw that goes from the lower left to upper right corner of the interval, or vice versa) (Figure 6b). While credible regions with boundaries that are non-monotonic (e.g., Argentina  $\times$  Innovator) have portions of the curve fit approximation that are poorer performing, the credible regions with monotonic boundaries (e.g., Minnesota  $\times$  Dakota Russet) seem to be satisfactory across the entire range of the curve.

**Table 1.** Paired critical N dilution curve parameters for each variety within location for the median value (CNDC) from the posterior distribution of the fitted hierarchical Bayesian model and the estimates for the credible region lower ( $CNDC_{lo}$ ) and upper ( $CNDC_{up}$ ) boundaries using the non-linear regression method.

Location	Variety	$CNDC_{lo}$		$CNDC$		$CNDC_{up}$	
		$a_{lo}$	$b_{lo}$	$a$	$b$	$a_{up}$	$b_{up}$
Argentina	Bannock Russet	4.82	0.146	4.96	0.140	5.10	0.135
	Gem Russet	4.80	0.190	4.96	0.178	5.07	0.152
	Innovator	4.83	0.241	4.94	0.212	5.06	0.193
	Markies Russet	4.82	0.167	4.96	0.155	5.08	0.135
	Umatilla Russet	4.85	0.195	4.95	0.165	5.06	0.143
Belgium	Bintje	4.52	0.606	4.72	0.579	4.90	0.567
	Charlotte	4.56	0.607	4.74	0.559	4.89	0.531
Canada	Russet Burbank	4.53	0.498	4.74	0.489	4.93	0.480
	Shepody	4.55	0.416	4.77	0.412	4.95	0.406
Minnesota	Clearwater	4.56	0.622	4.75	0.585	4.93	0.558
	Dakota Russet	4.54	0.619	4.75	0.599	4.94	0.588
	Easton	4.54	0.608	4.75	0.592	4.91	0.567
	Russet Burbank	4.51	0.562	4.74	0.566	4.95	0.567
	Umatilla Russet	4.56	0.631	4.75	0.588	4.92	0.546

However, the approximation of uncertainty in  $\%N_c$  based directly on uncertainty in CNDC parameters  $a$  and  $b$ , using the previously determined credible interval boundaries (Figure 3), were found to contain the entire credible region for all varieties within location evaluated (Figure 6a).

Therefore, this approach directly using the uncertainty in CNDC parameters is quite uninformative and should be used as a last resort to estimate %N<sub>c</sub> uncertainty when the credible region defined from either the original model fit or from the paired CNDC<sub>lo</sub> or CNDC<sub>up</sub> curves is unavailable. In the absence of the credible region defined directly from the fitted hierarchical Bayesian model, the CNDC<sub>lo</sub> and CNDC<sub>up</sub> (Table 7) are a suitable first-order representation of the credible region for %N<sub>c</sub>.

### 3.3. *Evaluating Differences between Critical N Concentration*

#### 3.3.1. Differences Related to $G \times E \times M$ Effects

While an evaluation of the pairwise differences between all varieties within location was conducted and is presented in the Supplemental Materials (Figure S2), a subset of the results comparing Minnesota  $\times$  Russet Burbank to all other varieties within location, Argentina  $\times$  Innovator to all other varieties within Argentina, Canada  $\times$  Russet Burbank to all other varieties within Canada, and Belgium  $\times$  Bintje to all other varieties within Belgium are presented in detail here (Figure 7).

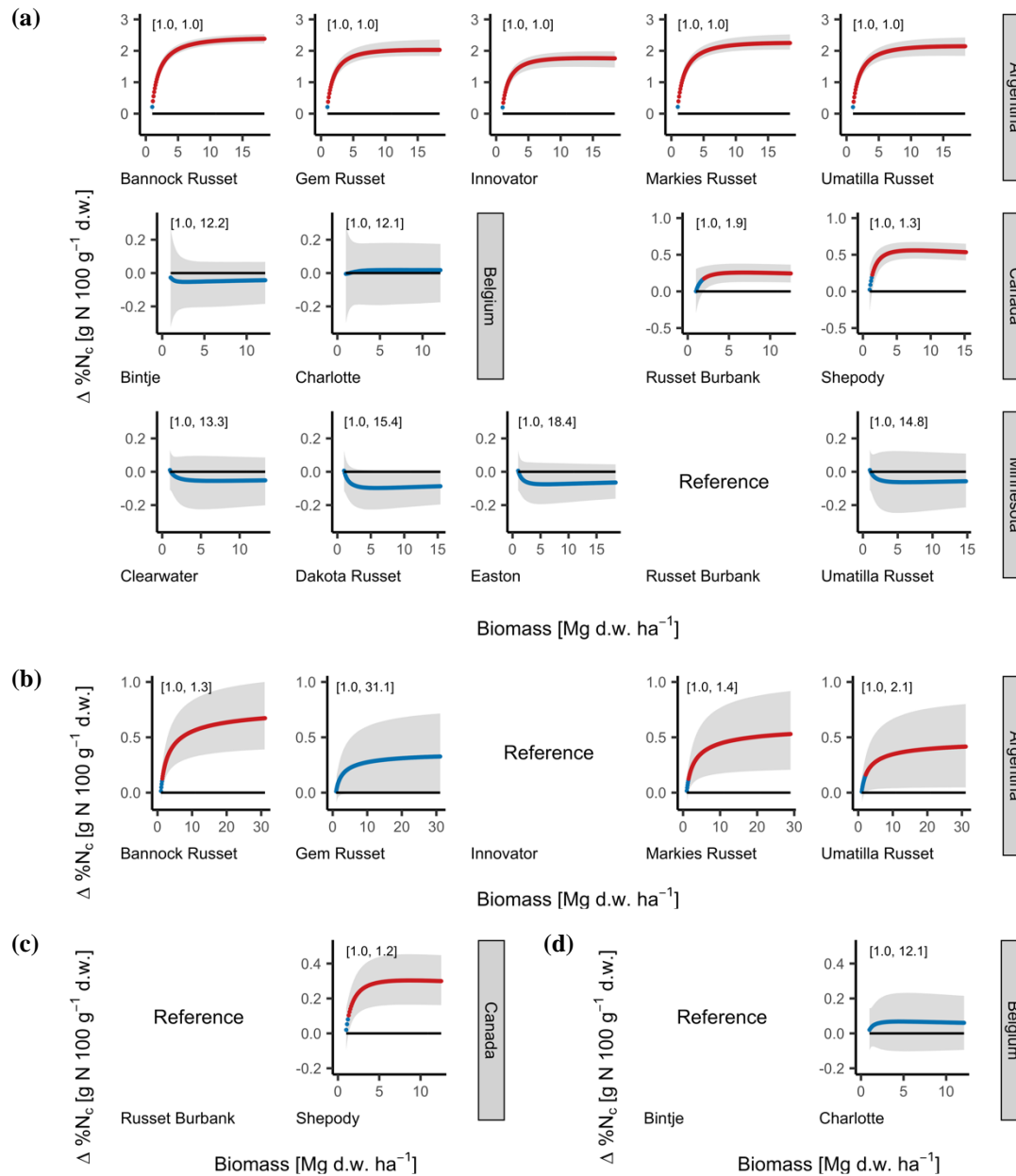


**Figure 5.** Comparison of the difference in critical N concentration values [ $\Delta\%N_c$ ] between (a) Minnesota  $\times$  Russet Burbank and all other varieties within location, (b) Argentina  $\times$  Innovator and all other varieties within Argentina, (c) Canada  $\times$  Russet Burbank and all other varieties within Canada, and (d) Belgium  $\times$  Bintje and all other varieties within Belgium for critical N concentration [ $\%N_c$ ] determined by the hierarchical Bayesian method. The grey shaded region represents the 90% credible region (lower bound, 0.05 quantile; upper bound, 0.95 quantile) for  $\Delta\%N_c$ . The colored points represent the median value for  $\Delta\%N_c$  at a given Biomass level where blue or red color respectively indicate that the credible region for  $\Delta\%N_c$  does or does not contain zero. The solid black line at constant  $\Delta\%N_c$  value of zero represents  $\%N_c$  for the reference curve (i.e., Minnesota  $\times$  Russet Burbank, Argentina  $\times$  Innovator, Canada  $\times$  Russet Burbank, and Belgium  $\times$  Bintje). The range of biomass values for which  $\Delta\%N_c$  is not significantly different (i.e., credible region contains zero) is given in brackets.

For Minnesota  $\times$  Russet Burbank, there were no significant differences in %N<sub>c</sub> for any level of W evaluated with any of the other varieties in Minnesota (i.e., Clearwater, Dakota Russet, Easton, and Umatilla Russet) or with the Belgium varieties (i.e., Bintje, and Charlotte) (Figure 7a). The %N<sub>c</sub> for both of the Canadian varieties (i.e., Russet Burbank, and Shepody) were significantly greater than that for Minnesota  $\times$  Russet Burbank when biomass values were greater than 2 Mg ha<sup>-1</sup> dry wt. The %N<sub>c</sub> for Canada  $\times$  Russet Burbank and Canada  $\times$  Shepody were up to 0.3 and 0.6 g N 100 g<sup>-1</sup> dry wt. greater than that for Minnesota  $\times$  Russet Burbank, respectively. The %N<sub>c</sub> for the Argentina varieties (i.e., Bannock Russet, Gem Russet, Innovator, Markies Russet, and Umatilla Russet) were significantly greater than for Minnesota  $\times$  Russet Burbank, except for at a biomass value of 1.0 Mg dry wt. ha<sup>-1</sup>, with a difference in value depending on variety of up to 2.4 g N 100 g<sup>-1</sup> dry wt.

For Argentina  $\times$  Innovator, %N<sub>c</sub> was significantly lower than for Argentina  $\times$  Bannock Russet, Argentina  $\times$  Markies Russet, and Argentina  $\times$  Umatilla Russet but was not significantly different from Argentina  $\times$  Gem Russet (Figure 7b). The %N<sub>c</sub> for Argentina  $\times$  Bannock Russet, Argentina  $\times$  Markies Russet, and Argentina  $\times$  Umatilla Russet were up to 0.5 g N 100 g<sup>-1</sup> dry wt. greater than that for Argentina  $\times$  Innovator. For Canada  $\times$  Russet Burbank, %N<sub>c</sub> was significantly lower than for Canada  $\times$  Shepody (Figure 7c), with a difference in %N<sub>c</sub> of up to 0.3 g N 100 g<sup>-1</sup> dry wt. For Belgium  $\times$  Bintje, %N<sub>c</sub> was not significantly different from Belgium  $\times$  Charlotte (Figure 7d).

There are two notable findings to point out. First, there were no significant differences between Minnesota  $\times$  Russet Burbank and any other varieties evaluated in Minnesota or between Belgium  $\times$  Bintje and the other variety evaluated in Belgium. This finding did not hold for all varieties within location evaluated, however; there were significant differences between varieties evaluated in both Argentina and Canada. Second, the comparison between the Minnesota  $\times$  Russet Burbank

and Canada × Russet Burbank curves as well as the comparison between the Minnesota × Umatilla Russet and Argentina × Umatilla (Figure S2) were both significantly different.

### 3.3.2. Differences Related to Statistical Methods

Comparing the curves fit in the present study with the Bayesian hierarchical method to the curves fit in the previous studies using conventional statistical methods, there were significant differences between statistical curve fit methods for all varieties within location evaluated (Figure 8). None of the previous CNDCs fall entirely within the credible region for the respective CNDCs developed in the present study.

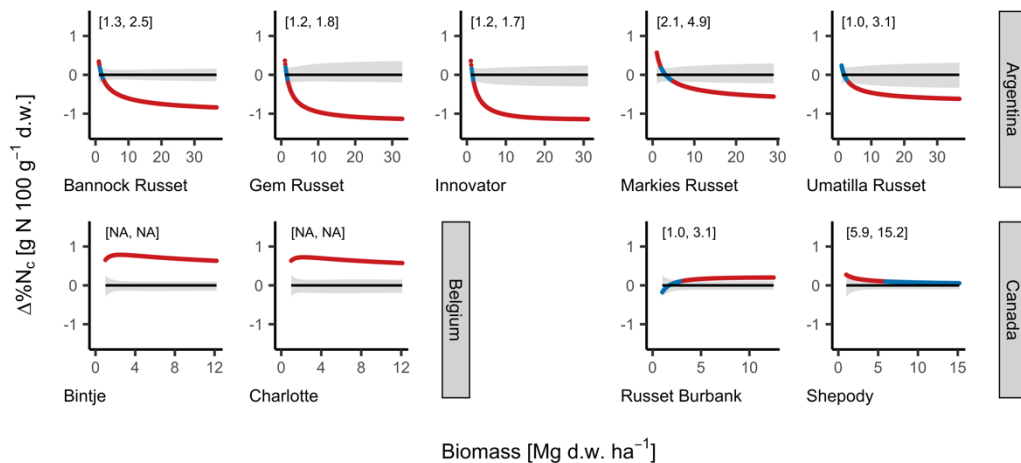


**Figure 6.** Comparison of the difference in critical N concentration values [ $\Delta\%N_c$ ] between the conventional statistical methods used in previous studies (i.e., Argentina – Giletto and Echeverría (2015); Belgium – Ben Abdallah et al. (2016); Canada – Bélanger et al. (2001a)) and the hierarchical Bayesian method used in the present study for each variety within location. The grey shaded region represents the 90% credible region (lower bound, 0.05 quantile; upper bound, 0.95 quantile) for critical N concentration [ $\%N_c$ ] from the hierarchical Bayesian method. The solid black line at a constant  $\Delta\%N_c$  value of zero represents the median value for  $\%N_c$  from the hierarchical Bayesian method. Red or blue points respectively indicate that  $\Delta\%N_c$  falls outside of (i.e., is significant) or falls within (i.e., is not significant) the 90% credible region for  $\%N_c$ . The range of biomass values for which  $\Delta\%N_c$  is not significant is given in brackets.

The  $\%N_c$  from the previously developed CNDCs for the Argentina varieties (Giletto & Echeverría, 2015) was significantly less than that from the present CNDCs across all varieties for biomass

levels of greater 5 Mg dry wt. ha<sup>-1</sup> (Figure 8). The magnitude of this difference was relatively large, with the  $\Delta\%N_c$  between the previous and present method ranging up to -0.6 to -1.1 g N 100 g<sup>-1</sup> dry wt., depending on variety. Therefore, relative to the statistical method used in this study it appears that the statistical methods used by Giletto and Echeverría (2015) selected biased critical points due to a overrepresentation of N limiting observations in the experimental dataset (Figure 5, Figure S1) leading to a systematic underestimation of  $\%N_c$ .

The  $\%N_c$  from the previously developed CNDCs for Belgium (Ben Abdallah et al., 2016) were significantly greater than that from the CNDCs developed in the present study (Figure 8). For all levels of biomass,  $\Delta\%N_c$  between the previous and present methods was significantly different with a value of 0.7 g N 100 g<sup>-1</sup> dry wt. Therefore, relative to the statistical method used in this study, it appears that the statistical methods used by Ben Abdallah et al. (2016) selected biased critical points due to overrepresentation of non-N limiting observations in the experimental dataset leading to a systematic overestimation of the  $\%N_c$ .

The  $\%N_c$  from the previously developed CNDCs for Canada (Bélanger et al., 2001a) was significantly greater for both Canada × Russet Burbank and Canada × Shepody than the present CNDCs for biomass levels of less than 3 Mg dry wt ha<sup>-1</sup> and greater than 6 Mg dry wt ha<sup>-1</sup>, respectively (Figure 8). Relative to the other locations, however, the CNDCs for Canada were the most similar between statistical methods, with small value for  $\Delta\%N_c$  of only 0.2 g N 100 g<sup>-1</sup> dry wt. Therefore, relative to the statistical method used in this study, it appears that the statistical method used by Bélanger et al. (2001a) did not select biased critical points likely due to the minimal bias observed in this experimental dataset.



Because a CNDC using the conventional statistical methods has not been previously published for potato in Minnesota, no comparison across statistical methods is made for this experimental dataset. However, the bias observed in the Minnesota experimental dataset is similar to the bias found in the Belgium experimental dataset; therefore, using the conventional statistical methods to derive a CNDC for Minnesota would likely overestimate %N<sub>c</sub> relative to the hierarchical Bayesian method.

## 4. Discussion

### 4.1. Mechanisms of Dilution

While the present study presents direct evidence of significant differences between CNDCs for potato across  $G \times E \times M$  effects, previous studies help describe the potential physiological mechanisms for this source of variation. Reviewing previous work on this topic, Lemaire et al. (2019) described a framework with which to consider the variation in relative partitioning of dry matter. First, relative partitioning varies as biomass varies over the growing season indicating that there is an ontogenetic relationship between harvest index and biomass. Second, the allometric trajectory of relative allocation (e.g., harvest index at a given level of biomass) is subject to variation in non-ontogenetic factors (i.e.,  $G \times E \times M$  interactions).

The findings of Giletto et al. (2020) suggest that the variation in CNDCs for potato are due to non-ontogenetic factors. In general,  $G \times E \times M$  interactions that result in greater and more rapid relative partitioning of biomass from vines (i.e., high N metabolic and structural tissue) to tubers (i.e., low N storage tissues) will result in greater N dilution (i.e., lower %N<sub>c</sub>) at the same level of total plant biomass (Lemaire et al., 2019). The two factors described by Giletto et al. (2020) affecting N

dilution due to non-ontogenetic factors are total plant biomass at tuber initiation (i.e., timing of tuber initiation) and relative rate of tuber growth to plant growth (i.e., relative rate of tube bulking). These two factors are affected by various physiological mechanisms and  $G \times E \times M$  interactions; however, relatively limited work has been conducted to comprehensively evaluate the combined effect of  $G \times E \times M$  interaction on these two physiological mechanisms for potato.

#### 4.1.1. Timing of Tuber Initiation

The timing of tuber initiation is affected primarily by variety maturity class (i.e., G). Potato varieties are classified on a spectrum of growth patterns where early maturing varieties are considered to be determinant and later maturing varieties are considered to be indeterminant (Thornton, 2020). Compared to indeterminant varieties, determinate varieties progress more quickly to the tuber initiation growth stage (i.e., at lower total plant biomass) and have a more rapid tuber bulking (i.e., biomass increase) with limited additional canopy and vine biomass growth (i.e., increased harvest index for a given level of biomass) (Kleinkopf et al., 1981). Therefore, it is expected that increasing earliness of maturity for a potato variety would result in an increase in N dilution.

In the present study, differences in maturity class between resulted in differences in  $\%N_c$ . For example, Argentina  $\times$  Innovator, which has an early to medium maturity class, had significantly lower  $\%N_c$  than Argentina  $\times$  Bannock Russet, Argentina  $\times$  Markies Russet, and Argentina  $\times$  Umatilla Russet, which have either a medium-late to late or late to very late maturity class; however, Argentina  $\times$  Gem Russet, which has a medium to late maturity class did not have a significantly different  $\%N_c$  from Argentina  $\times$  Innovator (Table 7). This finding supports the

hypothesis that varieties with an earlier maturity class (i.e., earlier tuber initiation) will have lower %N<sub>c</sub> (i.e., greater N dilution).

Timing of tuber initiation is also subject to  $G \times E \times M$  interactions. Ideal conditions for tuber initiation are moderate to low soil N availability, shorter day length, high light intensity, and cool nighttime temperatures (Ewing & Struik, 1992; Thornton, 2020); when N fertilizer management results in excessively high soil N availability (Kleinkopf et al., 1981), under conditions of reduced solar irradiance (Menzel, 1985), or when nighttime soil temperature are elevated (Slater, 1968; Kim & Lee, 2019), tuber initiation can be delayed. Therefore, both M effects that result in excessive early-season soil N availability (e.g., all N applied at planting in a soluble form) and E effects that result in increased solar irradiance or reduced nighttime temperatures (i.e., increased diurnal temperature difference) could result in an increase in N dilution.

However, due the limitation of the experimental studies (i.e., the effect of M was not systematically varied across a given  $G \times E$  interaction), it is not possible to directly assess the impact of diurnal temperature difference, solar radiation, or N fertilizer source and timing (Table 5) on the timing of tuber initiation and N dilution distinct from the combined effect of  $G \times E \times M$  interactions.

#### 4.1.2. Rate of Tuber Bulking

The rate of tuber bulking and allocation of biomass to tubers is subject to the effects of E. Conventionally, potential biomass production has been considered as the product of total solar radiation and radiation use efficiency (Monteith, 1977; Sinclair & Muchow, 1999) as has been successfully applied to potato (Allen & Scott, 1980). Previous studies have suggested that decreasing diurnal temperature difference results in a reduction in tuber bulking rate (i.e., radiation use efficiency), most likely as a result of increasing utilization of photosynthesis assimilates for

1  
2  
3  
4 661 maintenance (via increased respiration) as nighttime temperature increases (Benoit et al., 1986;  
5  
6 662 Bennett et al., 1991; Lizana et al., 2017); however, Kim & Lee (2019) did not observe any effect  
7  
8  
9 663 of increasing diurnal temperature difference on tuber bulking rate.

10  
11  
12 664 Given the limitation of the experimental studies (i.e., the effect of E was not systematically varied  
13  
14  
15 665 across a given G x M interaction), it is not possible to directly assess the impact of diurnal  
16  
17 666 temperature difference and solar radiation (Table 5) on the rate of tuber bulking across G x E x M  
18  
19  
20 667 interactions.

21  
22  
23 668 Planting density is an important effect of M that may play a key role in determining the relative  
24  
25  
26 669 partitioning of biomass for to tuber. Previous studies investigating this effect have found that as  
27  
28 670 planting density increases, leaf area index increases (Bremner & Taha, 1966; Ifenkwe & Allen,  
29  
30 671 1978; Allen & Scott, 1980), tuber dry weight biomass on a per area basis increases (Bremner &  
31  
32 672 Taha, 1966; Ifenkwe & Allen, 1978), while tuber dry weight biomass on a per plant basis decreases  
33  
34  
35 673 (Bremner & Taha, 1966; Ifenkwe & Allen, 1978). The combination of the effect of increasing  
36  
37  
38 674 planting density could plausibly result in the net effect of an increased relative proportion of  
39  
40 675 biomass allocated to vines (i.e., reduction in harvest index) (Vander Zaag et al., 1990), therefore  
41  
42  
43 676 reducing N dilution and resulting in increased %N<sub>c</sub>.

44  
45  
46 677 In the present study, variations in %N<sub>c</sub> due to variation in planting density were observed. For  
47  
48  
49 678 example, Argentina has the highest planting density of any location (Table 5) which resulted in  
50  
51 679 greater %N<sub>c</sub> than all other locations (Figure S2). The relative effect of planting density also appears  
52  
53  
54 680 to be of greater magnitude than other sources of variation (e.g., maturity class). For example,  
55  
56 681 Canada × Russet Burbank, which has a late to very late maturity class and planting density of  
57  
58  
59 682 29,000 plants ha<sup>-1</sup>, had a lower %N<sub>c</sub> than Canada × Shepody, which has a early to medium-early

maturity class and planting density of 44,000 plants ha<sup>-1</sup> (Table 5, Figure 7c). Therefore, this finding suggests that the effect of planting density (i.e., rate of tuber bulking) may be relatively more important at controlling %N<sub>c</sub> than the effect of maturity class (i.e., timing of tuber initiation). Because there was only a single level of M (e.g., planting density) within each level of G × E for the experimental trials considered here, additional experimental data is required to fully consider the independent effects of G, E, and M on critical N dilution. Therefore, future experimental studies explicitly investigating the effect of M (e.g., planting density) on %N<sub>c</sub> should be conducted to properly consider the combined effects the G × E × M interaction.

#### 4.1.3. Comparison to Other Crops

These findings contrasts somewhat with the previous studies evaluating G × E × M effects on %N<sub>c</sub>. Yao et al. (2021) found a similar magnitude of effect on %N<sub>c</sub> for both G and E effects for wheat in China; however, Yao et al. (2021) also reported an E effect where %N<sub>c</sub> for wheat in China was significantly different from that reported by Makowski et al. (2020) for wheat in France. Ciampitti et al. (2021) identified variation in %N<sub>c</sub> for maize as a result of G × M interactions due to variation in hybrid and planting density. Fernández et al. (2021) found that variation in %N<sub>c</sub> for tall fescue across G × E × M effects were negligible. In any case, the magnitude of the difference in %N<sub>c</sub> across G x E x M interactions reported by the previous studies for wheat, maize, and tall fescue (Makowski et al., 2020; Ciampitti et al., 2021; Fernández et al., 2021; Yao et al., 2021) is less than that was observed in the present study for potato.

Therefore, the impact of G × E × M on %N<sub>c</sub> is not only significant for potato, but is also of potentially much greater relative importance compared to other crops (e.g., wheat, maize, tall fescue). This is because the magnitude of variability in %N<sub>c</sub> due to G × E × M interactions found

in the present study is relatively greater for potato than other crops; however, further additional experimental data is needed to confirm that this finding is not an artifact of the statistical methods or limitations of experimental data used in the present study.

#### 4.2. *Implication of $G \times E$ Variation on N Use Efficiency*

Understanding and properly interpreting the impact of  $G \times E \times M$  effects on NUE is a critical goal necessary to improve N fertilizer use; however, this must be done while controlling for the effect of crop N status (Lemaire & Ciampitti, 2020). The previous findings of Bohman et al. (2021) demonstrated that interpreting NUE and its constituent component of N utilization efficiency [NUE] is directly related to the parameters of the CNDC through the critical N utilization efficiency curve [CNUtEC] which defines the critical value of NUE [NUE<sub>c</sub>]:

$$\text{NUE}_c = 1000 (10 a W^{-b})^{-1} \quad [8]$$

where parameters  $a$  and  $b$ , and  $W$  have the same meaning and units as previously defined in the present study and NUE<sub>c</sub> has units of g dry wt. g<sup>-1</sup> N. When NUE is greater than NUE<sub>c</sub>, crop N status is deficient (i.e., NNI less than 1); conversely, when NUE is less than NUE<sub>c</sub>, crop N status is excessive (i.e., NNI greater than 1).

The finding in the present study that the CNDC can vary across  $G \times E \times M$  interactions and the finding from Bohman et al. (2021) of the intrinsic relationship between NUE and the CNDC together lead to the conclusion that the CNUtEC must also vary across the same  $G \times E \times M$  effects as the CNDC. Therefore, the effect of  $G \times E \times M$  on variation of NUE<sub>c</sub> is one of the multiple set of factors that ultimately control NUE. Understanding and accounting for the  $G \times E \times M$  effect on the CNUtEC is therefore critically important to understand the impacts of  $G \times E \times M$  interactions

on NUE. In other words, controlling for this  $G \times E \times M$  effect represents an additional requirement when evaluating and interpreting NUE above and beyond the previously known requirements of controlling for both NNI and biomass (Barraclough et al., 2010; Caviglia et al., 2014; Sadras & Lemaire, 2014; Gastal et al., 2015; Lemaire & Ciampitti, 2020).

Following from the above discussion of the CNUtEC and the findings of Giletto et al. (2020),  $G \times E \times M$  effects that increase the relative proportion of biomass partitioned to tubers and reduce the time to tuber initiation will both decrease the  $\%N_c$  and increase the  $NUtE_c$  values. Therefore, future efforts to systematically improve NUE in potato through either management practices (e.g., Bohman et al. (2021)) or crop breeding (e.g., Tiwari et al. (2018); Jones et al. (2021); Stefaniak et al. (2021)) should focus on identifying  $G \times E \times M$  interactions that result in an increased proportion of biomass partitioned to tubers or result in earlier timing of tuber initiation.

### 4.3. *Uncertainty in Critical N Concentration*

#### 4.3.1. Communicating Uncertainty in Critical N Concentration

This study as well as others that implemented Bayesian statistical methods to derive critical N dilution curves (Makowski et al., 2020; Ciampitti et al., 2021; Yao et al., 2021) clearly indicate that there is meaningful uncertainty in  $\%N_c$  values. Therefore, the use of  $\%N_c$  in subsequent calculations should include this inherent uncertainty. However, the direct use of the credible region defined from posterior distribution of the fitted Bayesian hierarchical model in subsequent calculations is impractical, and a method to concisely and accurately communicate the credible region remains necessary.

Our finding that the credible region can be satisfactorily estimated using an equation of the same form as the CNDC (Figure 6) suggests that an additional pair of negative exponential curves representing the upper and lower boundary of the credible region for %N<sub>c</sub> (i.e., CNDC<sub>lo</sub> and CNDC<sub>up</sub>) should be reported in future studies. In this manner, the median value and credible region for %N<sub>c</sub> is defined by a set of three, two-parameter curves (i.e., CNDC – *a*, *b*; CNDC<sub>up</sub> – *a*<sub>up</sub>, *b*<sub>up</sub>; CNDC<sub>lo</sub> – *a*<sub>lo</sub>, *b*<sub>lo</sub>) which can be easily communicated and used in subsequent computations (Table 7).

#### 4.3.2. Computing Uncertainty of Derived Parameters

Critical N concentration and the associated CNDC parameters are commonly used to derive and calculate other related parameters. For example, the calculation of NNI depends on both %N<sub>Plant</sub> and %N<sub>c</sub>. (Eq. [1] and Eq. [2]). However, to properly account for the uncertainty in %N<sub>c</sub> when computing NNI, the upper [%N<sub>c,up</sub>] and lower [%N<sub>c,lo</sub>] bounds of the credible interval for %N<sub>c</sub> should also be used to determine the upper [NNI<sub>up</sub>] and lower [NNI<sub>lo</sub>] bounds of the credible interval for NNI, where %N<sub>c,up</sub> and %N<sub>c,lo</sub> are calculated using the CNDC<sub>up</sub> and CNDC<sub>lo</sub>, respectively:

$$NNI_{up} = \%N_{Plant} / \%N_{c,up} = \%N_{Plant} / (a_{up} W^{-b_{up}}) \quad [9]$$

$$NNI_{lo} = \%N_{Plant} / \%N_{c,lo} = \%N_{Plant} / (a_{lo} W^{-b_{lo}}) \quad [10]$$

This has important practical implications for interpreting NNI values. For example, in a case where NNI is less than 1 but NNI<sub>up</sub> is greater than 1, it follows that crop N status would not be considered deficient (i.e., NNI is not significantly different from 1). In contrast, when both NNI and NNI<sub>lo</sub> are greater than 1, it follows that crop N status would be considered surplus (i.e., NNI is significantly



greater than 1). However, the threshold for considering significant differences in NNI will necessarily depend upon the threshold used for calculating  $\%N_{c,lo}$  and  $\%N_{c,up}$  (e.g., 90% confidence region). The conclusions of a small-plot trial evaluating the effect of various N fertilizer treatments on yield and biomass (e.g., Bohman et al. (2021)) may draw different conclusions when uncertainty in calculated NNI values is explicitly considered.

Additionally, the parameters of the CNDC (i.e.,  $a$ ,  $b$ ) are also used to parameterize other related curves such as the critical N uptake curve [CNUC] or the critical N utilization efficiency curve [CNUtEC] (Bohman et al., 2021). When computing the critical N uptake [ $N_c$ ] or critical N utilization efficiency [NUE<sub>c</sub>] values defined by these curves, respectively, the parameters from the CNDC<sub>lo</sub> (i.e.,  $a_{lo}$ ,  $b_{lo}$ ) and CNDC<sub>up</sub> (i.e.,  $a_{up}$ ,  $b_{up}$ ) should be used to calculate the upper and lower bounds of these derived values. In general, any calculation depending on either  $\%N_c$  or any equation that uses the parameters of the CNDC, should also additionally use the CNDC<sub>lo</sub> and CNDC<sub>up</sub> to account for uncertainty in  $\%N_c$ .

#### 4.4. Evaluating Differences between Statistical Methods

While the occurrence of difference in CNDCs derived using the Bayesian hierarchical model compared to the conventional statistical methods (Figure 7) is itself notable, the magnitude of the differences found in the present study is especially remarkable. Because of its strong theoretical underpinning,  $\%N_c$  and NNI are typically considered to be high fidelity measurements of crop N status, not affected by the subjectivity or relativity found in most other methods (Lemaire et al., 2019). However, the findings of the present study strongly suggest that this conception of the NNI framework must be qualified within a particular application by the statistical methods used to derive the CNDC for a given experimental dataset. Additionally, having sufficient quantity and

quality of experimental data to derive a CNDC remains an essential criteria to consider (Fernández et al., 2021), in addition to the statistical methods used.

Unfortunately, the direct evaluation of different statistical methods to calculate the CNDC from the same experimental dataset cannot directly answer the question of which statistical method or resulting CNDC is “correct” (i.e., most accurate, least biased). However, we can reasonably conclude from both deduction and from the findings of the present study that a Bayesian hierarchical model utilizing the linear-plateau method and leveraging partial pooling across effect levels will result in inference that is less subjected to potential bias in the experimental data set compared to the conventional statistical methods. Additionally, it extracts the greatest amount of information from a given dataset, as no data are excluded from the fitting of the total model.

Therefore, it appears preferable for the future development of CNDCs to utilize the Bayesian hierarchical method to both quantify uncertainty and reduce bias in %N<sub>c</sub>. Without addressing these limitations (i.e., bias and uncertainty), both directly resulting from the statistical methods used, the NNI framework cannot fulfill its core objective of providing an absolute reference of crop N status.

Additionally, with further development of adequate tools for this scientific computing task, the implementation of the Bayesian hierarchical framework for deriving the CNDC can be made trivial and may enable the development of CNDCs from existing but unutilized experimental datasets. Therefore, the development of a dedicated software library to implement the Bayesian hierarchical method is a priority for future research efforts. Developing standardized tools to implement the partially-pooled Bayesian hierarchical method will enable more widespread implementation of this preferred method to derive CNDCs.

## 5. Conclusions

First, this study demonstrated that there are significant differences between CNDCs developed across  $G \times E \times M$  effects for potato. Therefore, any application of  $\%N_c$  must use an appropriate CNDC (i.e., not significantly different) for the  $G \times E \times M$  interaction being considered. Second, this study developed an approach to communicate uncertainty in  $\%N_c$  through the concise set of six parameters defined by the CNDC (i.e.,  $a$ ,  $b$ ),  $CNDC_{lo}$  (i.e.,  $a_{lo}$ ,  $b_{lo}$ ), and  $CNDC_{up}$  (i.e.,  $a_{up}$ ,  $b_{up}$ ), and the  $\%N_c$  value computed from these three curves should be used in all subsequent computations to propagate uncertainty. Third, this study demonstrated that the statistical method used to derive CNDCs affects the inferred  $\%N_c$  values, and that the partially-pooled hierarchical Bayesian framework is less susceptible to bias due to biased experimental data than the conventional statistical methods. Therefore, future efforts to derive CNDCs should utilize the partially-pooled hierarchical Bayesian framework whenever possible. Fourth, the findings of this study suggest that variation in  $\%N_c$  across  $G \times E \times M$  interactions necessarily extends to NUE, via the relationship between the CNDC and the  $CNU_{tEC}$ . Therefore, NUE is dependent on the mechanisms that control N dilution (i.e., biomass partitioning), and future efforts to improve NUE should explicitly consider how  $G \times E \times M$  interactions affect N dilution.

1  
2  
3  
4 **6. Acknowledgements**  
5

6  
7 828 Research funding for this project was provided by Minnesota Area II Potato Growers Research  
8 829 and Promotion Council, and the Clean Water Land and Legacy Amendment with funding  
9 830 administered through the Minnesota Department of Agriculture.  
10 831  
11  
12  
13  
14  
15  
16  
17  
18  
19  
20  
21  
22  
23  
24  
25  
26  
27  
28  
29  
30  
31  
32  
33  
34  
35  
36  
37  
38  
39  
40  
41  
42  
43  
44  
45  
46  
47  
48  
49  
50  
51  
52  
53  
54  
55  
56  
57  
58  
59  
60  
61  
62  
63  
64  
65

## 7. References

- AHDB. (2015). Charlotte: Agriculture and Horticulture Development Board. Retrieved from <https://varieties.ahdb.org.uk/varieties/view/CHARLOTTE>
- Allen, E.J., and R.K. Scott. (1980). An Analysis of Growth of the Potato Crop. *J. Agr. Sci.*, 94(3), 583-606. <https://doi.org/10.1017/S0021859600028598>.
- Barracough, P.B., J.R. Howarth, J. Jones, R. Lopez-Bellido, S. Parmar, C.E. Shepherd, and M.J. Hawkesford. (2010). Nitrogen Efficiency of Wheat: Genotypic and Environmental Variation and Prospects for Improvement. *Eur. J. Agron.*, 33(1), 1-11. <https://doi.org/10.1016/j.eja.2010.01.005>.
- Bates, D.M. (2010). *Lme4: Mixed-Effects Modeling with R*.
- Bélanger, G., J.R. Walsh, J.E. Richards, P.H. Milburn, and N. Ziadi. (2000). Yield Response of Two Potato Cultivars to Supplemental Irrigation and N Fertilization in New Brunswick. *Am. J. Potato Res.*, 77(1), 11-21. <https://doi.org/10.1007/BF02853657>.
- Bélanger, G., J.R. Walsh, J.E. Richards, P.H. Milburn, and N. Ziadi. (2001a). Critical Nitrogen Curve and Nitrogen Nutrition Index for Potato in Eastern Canada. *Am. J. Potato Res.*, 78(5), 355-364. <https://doi.org/10.1007/BF02884344>.
- Bélanger, G., J.R. Walsh, J.E. Richards, P.H. Milburn, and N. Ziadi. (2001b). Tuber Growth and Biomass Partitioning of Two Potato Cultivars Grown under Different N Fertilization Rates with and without Irrigation. *Am. J. Potato Res.*, 78(2), 109-117. <https://doi.org/10.1007/BF02874766>.
- Ben Abdallah, F., M. Olivier, J.P. Goffart, and O. Minet. (2016). Establishing the Nitrogen Dilution Curve for Potato Cultivar Bintje in Belgium. *Potato Res.*, 59(3), 241-258. <https://doi.org/10.1007/s11540-016-9331-y>.
- Bennett, S.M., T.W. Tibbitts, and W. Cao. (1991). Diurnal Temperature Fluctuation Effects on Potatoes Grown with 12 Hr Photoperiods. *Am. Potato J.*, 68, 81-86. <https://doi.org/10.1007/BF02853925>.
- Benoit, G.R., W.J. Grant, and O.J. Devine. (1986). Potato Top Growth as Influenced by Day-Night Temperature Differences. *Agron. J.*, 78(2), 264-269. <https://doi.org/10.2134/agronj1986.00021962007800020010x>.
- Bohman, B.J., M. McNearney, J. Crants, and C.J. Rosen. (2020). A Novel Approach to Manage Nitrogen Fertilizer for Potato Production Using Remote Sensing. *Research Reports – 2020*. Fargo, ND: Minnesota Area II Potato Research and Promotion Council and Northern Plains Potato Growers Association. Retrieved from <https://www.ag.ndsu.edu/potatoextension/research/2020ResearchBooks.pdf>
- Bohman, B.J., C.J. Rosen, and D.J. Mulla. (2021). Relating Nitrogen Use Efficiency to Nitrogen Nutrition Index for Evaluation of Agronomic and Environmental Outcomes in Potato. *Field Crops Res.*, 262. <https://doi.org/10.1016/j.fcr.2020.108041>.
- Bremner, P.M., and M.A. Taha. (1966). Studies in Potato Agronomy. I. The Effects of Variety, Seed Size and Spacing on Growth, Development and Yield. *The Journal of Agricultural Science*, 66(2), 241-252. <https://doi.org/10.1017/s0021859600062651>.
- Bürkner, P.-C. (2017). Brms: An R Package for Bayesian Multilevel Models Using Stan. *J. Stat. Softw.*, 80(1). <https://doi.org/10.18637/jss.v080.i01>.
- Bürkner, P.-C. (2018). Advanced Bayesian Multilevel Modeling with the R Package Brms. *R J.*, 10(1), 395-411. <https://doi.org/10.32614/RJ-2018-017>.

- Carpenter, B., A. Gelman, M.D. Hoffman, D. Lee, B. Goodrich, M. Betancourt, M. Brubaker, J. Guo, P. Li, and A. Riddell. (2017). Stan: A Probabilistic Programming Language. *J. Stat. Softw.*, 76(1). <https://doi.org/10.18637/jss.v076.i01>.
- Caviglia, O.P., R.J.M. Melchiori, and V.O. Sadras. (2014). Nitrogen Utilization Efficiency in Maize as Affected by Hybrid and N Rate in Late-Sown Crops. *Field Crops Res.*, 168, 27-37. <https://doi.org/10.1016/j.fcr.2014.08.005>.
- CFIA. (2013). Bintje: Canadian Food Inspection Agency. Retrieved from <https://inspection.canada.ca/plant-varieties/potatoes/potato-varieties/bintje/eng/1312587385655/1312587385656>
- Ciampitti, I.A., J. Fernandez, S. Tamagno, B. Zhao, G. Lemaire, and D. Makowski. (2021). Does the Critical N Dilution Curve for Maize Crop Vary across Genotype X Environment X Management Scenarios? - a Bayesian Analysis. *Eur. J. Agron.*, 123, 126202. <https://doi.org/10.1016/j.eja.2020.126202>.
- Crants, J., C. Rosen, M. McNearney, and L. Sun. (2017). The Use of Chlorophyll Meters for Nitrogen Management in Potatoes. *Research Reports – 2017*. Fargo, ND: Minnesota Area II Potato Research and Promotion Council and Northern Plains Potato Growers Association. Retrieved from <https://www.ag.ndsu.edu/potatoextension/research>
- Duchenne, T., J.M. Machet, and M. Martin. (1997). Potatoes. In G. Lemaire (Ed.), *Diagnosis of the Nitrogen Status in Crops* (pp. 119-130). Berlin: Springer.
- Egel, D.S. (2017). Midwest Vegetable Production Guide for Commercial Growers. *BU-07094-S*: University of Minnesota Extension. Retrieved from <https://ag.purdue.edu/btny/midwest-vegetable-guide/Pages/default.aspx>
- Errebhi, M., C.J. Rosen, S.C. Gupta, and D.E. Birong. (1998). Potato Yield Response and Nitrate Leaching as Influenced by Nitrogen Management. *Agron. J.*, 90, 10-15. <https://doi.org/10.2134/agronj1998.00021962009000010003x>.
- Ewing, E.E., and P.C. Struik. (1992). Tuber Formation in Potato: Induction, Initiation, and Growth. In J. Janick (Ed.), *Horticultural Reviews, Volume 14* (pp. 89-198): John Wiley & Sons.
- Fernández, J.A., G. Lemaire, G. Bélanger, F. Gastal, D. Makowski, and I.A. Ciampitti. (2021). Revisiting the Critical Nitrogen Dilution Curve for Tall Fescue: A Quantitative Synthesis. *Eur. J. Agron.*, 131, 126380. <https://doi.org/10.1016/j.eja.2021.126380>.
- Franzen, D., A. Robinson, and C. Rosen. (2018). Fertilizing Potato in North Dakota. *SF715*. Fargo, ND: North Dakota State University. Retrieved from <https://www.ag.ndsu.edu/publications/crops/fertilizing-potato-in-north-dakota>
- Gastal, F., G. Lemaire, J.-L. Durand, and G. Louarn. (2015). Quantifying Crop Responses to Nitrogen and Avenues to Improve Nitrogen-Use Efficiency. In *Crop Physiology* (Second ed., pp. 161-206).
- Gelaro, R., W. McCarty, M.J. Suarez, R. Todling, A. Molod, L. Takacs, C. Randles, A. Darmanov, M.G. Bosilovich, R. Reichle, K. Wargan, L. Coy, R. Cullather, C. Draper, S. Akella, V. Buchard, A. Conaty, A. da Silva, W. Gu, G.K. Kim, R. Koster, R. Lucchesi, D. Merkova, J.E. Nielsen, G. Partyka, S. Pawson, W. Putman, M. Rienecker, S.D. Schubert, M. Sienkiewicz, and B. Zhao. (2017). The Modern-Era Retrospective Analysis for Research and Applications, Version 2 (Merra-2). *J. Clim.*, Volume 30(Iss 13), 5419-5454. <https://doi.org/10.1175/JCLI-D-16-0758.1>.
- Giletto, C.M., and H.E. Echeverría. (2015). Critical Nitrogen Dilution Curve in Processing Potato Cultivars. *Am. J. Plant Sci.*, 06(19), 3144-3156. <https://doi.org/10.4236/ajps.2015.619306>.

- Giletto, C.M., N.I. Reussi Calvo, P. Sandaña, H.E. Echeverría, and G. Bélanger. (2020). Shoot- and Tuber-Based Critical Nitrogen Dilution Curves for the Prediction of the N Status in Potato. *Eur. J. Agron.*, 119. <https://doi.org/10.1016/j.eja.2020.126114>.
- Greenwood, D.J., G. Lemaire, G. Gosse, P. Cruz, A. Draycott, and J.J. Neeteson. (1990). Decline in Percentage N of C3 and C4 Crops with Increasing Plant Mass. *Ann. Bot.*, 66(4), 425-436. <https://doi.org/10.1093/oxfordjournals.aob.a088044>.
- Greenwood, D.J., J.J. Neeteson, and A. Draycott. (1986). Quantitative Relationships for the Dependence of Growth Rate of Arable Crops on Their Nitrogen Content, Dry Weight and Aerial Environment. *Plant Soil*, 91(3), 281-301. <https://doi.org/10.1007/BF02198111>.
- Gupta, S., and C.J. Rosen. (2019). Nitrogen Fertilization Rate and Cold-Induced Sweetening in Potato Tubers During Storage. *Research Reports – 2019*. Fargo, ND: Minnesota Area II Potato Research and Promotion Council and Northern Plains Potato Growers Association. Retrieved from <https://www.ag.ndsu.edu/potatoextension/research/2019RESEARCHREPORTS.pdf>
- Gupta, S.K., J. Crants, M. McNearney, and C.J. Rosen. (2020). Evaluation of a Promising Minnesota Clone for N Response, Agronomic Traits & Storage Quality. *Research Reports – 2020*. Fargo, ND: Minnesota Area II Potato Research and Promotion Council and Northern Plains Potato Growers Association. Retrieved from <https://www.ag.ndsu.edu/potatoextension/research/2020ResearchBooks.pdf>
- Hansen, B., and A.G. Giencke. (1988). Sand Plains Research Farm Soil Report. St. Paul, MN: University of Minnesota
- Herrmann, A., and F. Taube. (2004). The Range of the Critical Nitrogen Dilution Curve for Maize (*Zea Mays* L.) Can Be Extended until Silage Maturity. *Agron. J.*, 96(4), 1131-1138. <https://doi.org/10.2134/agronj2004.1131>.
- Horneck, D.A., and R.O. Miller. (1998). Determination of Total Nitrogen in Plant Tissue. In Y. P. Kalra (Ed.), *Handbook of Reference Methods for Plant Analysis* (pp. 75-84). Boston: CRC Press.
- Horwitz, W., P. Chichilo, and H. Reynolds. (1970). *Official Methods of Analysis of the Association of Official Analytical Chemists*. (11th ed.). Washington, DC: Association of Official Analytical Chemists.
- Houlès, V., M. Guérif, and B. Mary. (2007). Elaboration of a Nitrogen Nutrition Indicator for Winter Wheat Based on Leaf Area Index and Chlorophyll Content for Making Nitrogen Recommendations. *Eur. J. Agron.*, 27(1), 1-11. <https://doi.org/10.1016/j.eja.2006.10.001>.
- Ifenkwe, O.P., and E.J. Allen. (1978). Effects of Row Width and Planting Density on Growth and Yield of Two Maincrop Potato Varieties. 1. Plant Morphology and Dry-Matter Accumulation. *The Journal of Agricultural Science*, 91(2), 265-278. <https://doi.org/10.1017/s0021859600046359>.
- Jones, C.R., T.E. Michaels, C.S. Carley, C.J. Rosen, and L.M. Shannon. (2021). Nitrogen Uptake and Utilization in Advanced Fresh-Market Red Potato Breeding Lines. *Crop Sci.*, 61, 878–895. <https://doi.org/10.1002/csc2.20297>.
- Justes, E., B. Mary, J.-M. Meynard, J.-M. Machet, and L. Thelier-Huche. (1994). Determination of a Critical Nitrogen Dilution Curve for Winter Wheat Crops. *Ann. Bot.*, 74(4), 397-407. <https://doi.org/10.1006/anbo.1994.1133>.
- Kim, Y.U., and B.W. Lee. (2019). Differential Mechanisms of Potato Yield Loss Induced by High Day and Night Temperatures During Tuber Initiation and Bulking: Photosynthesis and Tuber Growth. *Front. Plant Sci.*, 10, 300. <https://doi.org/10.3389/fpls.2019.00300>.

- Kleinkopf, G.E., D.T. Westermann, and R.B. Dwelle. (1981). Dry Matter Production and Nitrogen Utilization by Six Potato Cultivars. *Agron. J.*, 73(5), 799-802. <https://doi.org/10.2134/agronj1981.00021962007300050013x>.
- Lemaire, G., and I. Ciampitti. (2020). Crop Mass and N Status as Prerequisite Covariables for Unraveling Nitrogen Use Efficiency across Genotype-by-Environment-by-Management Scenarios: A Review. *Plants*, 9(10). <https://doi.org/10.3390/plants9101309>.
- Lemaire, G., and F. Gastal. (1997). N Uptake and Distribution in Plant Canopies. In G. Lemaire (Ed.), *Diagnosis of the Nitrogen Status in Crops* (pp. 3-43). Berlin: Springer.
- Lemaire, G., T. Sinclair, V. Sadras, and G. Bélanger. (2019). Allometric Approach to Crop Nutrition and Implications for Crop Diagnosis and Phenotyping. A Review. *Agron. Sustain. Dev.*, 39(2). <https://doi.org/10.1007/s13593-019-0570-6>.
- Li, D., Y. Miao, S.K. Gupta, C.J. Rosen, F. Yuan, C. Wang, L. Wang, and Y. Huang. (2021). Improving Potato Yield Prediction by Combining Cultivar Information and Uav Remote Sensing Data Using Machine Learning. *Remote Sens.*, 13(16). <https://doi.org/10.3390/rs13163322>.
- Lindstrom, M.J., and D.M. Bates. (1990). Nonlinear Mixed Effects Models for Repeated Measures Data. *Biometrics*, 46(3), 673-687. <https://doi.org/10.2307/2532087>.
- Lizana, X.C., A. Avila, A. Tolaba, and J.P. Martinez. (2017). Field Responses of Potato to Increased Temperature During Tuber Bulking: Projection for Climate Change Scenarios, at High-Yield Environments of Southern Chile. *Agric. For. Meteorol.*, 239, 192-201. <https://doi.org/10.1016/j.agrformet.2017.03.012>.
- Makowski, D., B. Zhao, S.T. Ata-Ul-Karim, and G. Lemaire. (2020). Analyzing Uncertainty in Critical Nitrogen Dilution Curves. *Eur. J. Agron.*, 118. <https://doi.org/10.1016/j.eja.2020.126076>.
- McElreath, R. (2020). *Statistical Rethinking: A Bayesian Course with Examples in R and Stan* (2nd ed.). Boca Raton: Chapman and Hall/CRC.
- Menzel, C.M. (1985). Tuberization in Potato at High Temperatures: Interaction between Temperature and Irradiance. *Ann. Bot.*, 55(1), 35-39. <https://doi.org/10.1093/oxfordjournals.aob.a086875>.
- Monteith, J.L. (1977). Climate and the Efficiency of Crop Production in Britain. *Phil. Trans. R. Soc. Lond. B*, 281, 277-294. <https://doi.org/10.1098/rstb.1977.0140>.
- Morier, T., A.N. Cambouris, and K. Chokmani. (2015). In-Season Nitrogen Status Assessment and Yield Estimation Using Hyperspectral Vegetation Indices in a Potato Crop. *Agron. J.*, 107(4), 1295-1309. <https://doi.org/10.2134/agronj14.0402>.
- Morris, T.F., T.S. Murrell, D.B. Beegle, J.J. Camberato, R.B. Ferguson, J. Grove, Q. Ketterings, P.M. Kyveryga, C.A.M. Laboski, J.M. McGrath, J.J. Meisinger, J. Melkonian, B.N. Moebius-Clune, E.D. Nafziger, D. Osmond, J.E. Sawyer, P.C. Scharf, W. Smith, J.T. Spargo, H.M. van Es, and H. Yang. (2018). Strengths and Limitations of Nitrogen Rate Recommendations for Corn and Opportunities for Improvement. *Agron. J.*, 110(1), 1. <https://doi.org/10.2134/agronj2017.02.0112>.
- Nigon, T.J., C. Yang, D.J. Mulla, and D.E. Kaiser. (2019). Computing Uncertainty in the Optimum Nitrogen Rate Using a Generalized Cost Function. *Comput. Electron. Agric.*, 167, 105030. <https://doi.org/10.1016/j.compag.2019.105030>.
- OSU. (2021). Potato Variety Identification and Ownership Table: Oregon State University – Oregon Seed Certification Service. Retrieved from




- [https://seedcert.oregonstate.edu/sites/seedcert.oregonstate.edu/files/potato\\_varietyratingkey.pdf](https://seedcert.oregonstate.edu/sites/seedcert.oregonstate.edu/files/potato_varietyratingkey.pdf)
- Plénet, D., and G. Lemaire. (2000). Relationships between Dynamics of Nitrogen Uptake and Dry Matter Accumulation in Maize Crops. Determination of Critical N Concentration. *Plant Soil*, 216(1/2), 65-82. <https://doi.org/10.1023/a:1004783431055>.
- Plummer, M. (2013). Jags: Just Another Gibbs Sampler. Retrieved from <http://mcmc-jags.sourceforge.net/>.
- Plummer, M. (2019). Rjags: Bayesian Graphical Models Using Mcmc. Retrieved from <https://CRAN.R-project.org/package=rjags>
- Porter, G. (2014). 201400091. USDA PVPO.
- R Core Team. (2021a). R: A Language and Environment for Statistical Computing. Vienna, Austria: R Foundation for Statistical Computing. Retrieved from <https://www.R-project.org/>
- R Core Team. (2021b). "Stats": The R Stats Package. Retrieved from <https://CRAN.R-project.org/package=stats>
- Rosen, C., D. Birong, and M. Zumwinkle. (1992). Nitrogen Fertilization Studies on Irrigated Potatoes: Nitrogen Use, Soil Nitrate Movement, and Petiole Sap Nitrate Analysis for Predicting Nitrogen Needs. *Field Research in Soil Science – Soil Series #134*. St. Paul, MN: University of Minnesota. Retrieved from <https://conservancy.umn.edu/handle/11299/121705>
- Rosen, C., J. Crants, B. Bohman, and M. McNearney. (2021). Effects of Banded Versus Broadcast Application of Esn, Turkey Manure, and Different Approaches to Measuring Plant N Status on Tuber Yield and Quality in Russet Burbank Potatoes. *Reserach Reports – 2021*. Fargo, ND: Minnesota Area II Potato Research and Promotion Council and Northern Plains Potato Growers Association. Retrieved from [https://www.ag.ndsu.edu/potatoextension/research/research\\_reports\\_114\\_4126022392.pdf](https://www.ag.ndsu.edu/potatoextension/research/research_reports_114_4126022392.pdf)
- Rosen, C., M. Errebhi, J. Moncrief, S. Gupta, H.H. Cheng, and D. Birong. (1993). Nitrogen Fertilization Studies on Irrigated Potatoes: Nitrogen Use, Soil Nitrate Movement, and Petiole Sap Nitrate Analysis for Predicting Nitrogen Needs. *Field Research in Soil Science – Soil Series #136*. St. Paul, MN: University of Minnesota. Retrieved from <https://conservancy.umn.edu/handle/11299/121706>
- Rosen, C.J. (2018). Potato Fertilization on Irrigated Soils: University of Minnesota Extension. Retrieved from <https://extension.umn.edu/crop-specific-needs/potato-fertilization-irrigated-soils>
- Sadras, V.O., and G. Lemaire. (2014). Quantifying Crop Nitrogen Status for Comparisons of Agronomic Practices and Genotypes. *Field Crops Res.*, 164, 54-64. <https://doi.org/10.1016/j.fcr.2014.05.006>.
- Schad, D.J., M. Betancourt, and S. Vasishth. (2021). Toward a Principled Bayesian Workflow in Cognitive Science. *Psychol Methods*, 26(1), 103-126. <https://doi.org/10.1037/met0000275>.
- Sinclair, T.R., and R.C. Muchow. (1999). Radiation Use Efficiency. In D. L. Sparks (Ed.), *Advances in Agronomy, Volume 65* (Vol. 65, pp. 215-265).
- Slater, J.W. (1968). The Effect of Night Temperature on Tuber Initiation of the Potato. *European Potato Journal*, 11(1), 14-22. <https://doi.org/10.1007/BF02365158>.
- Stark, J.C., A.L. Thompson, R. Novy, and S.L. Love. (2020). Variety Selection and Management. In J. C. Stark, M. Thornton, and P. Nolte (Eds.), *Potato Production Systems* (pp. 35-64).

- Steele, D.D., T.F. Scherer, J. Wright, D.G. Hopkins, S.R. Tuscherer, and J. Wright. (2010). Spreadsheet Implementation of Irrigation Scheduling by the Checkbook Method for North Dakota and Minnesota. *Appl. Eng. Agric.*, 26, 983-996. <https://doi.org/10.13031/2013.35914>.
- Stefaniak, T.R., S. Fitzcollins, R. Figueroa, A.L. Thompson, C. Schmitz Carley, and L.M. Shannon. (2021). Genotype and Variable Nitrogen Effects on Tuber Yield and Quality for Red Fresh Market Potatoes in Minnesota. *Agronomy*, 11, 255. <https://doi.org/10.3390/agronomy11020255>.
- Sun, N. (2017). *Agronomic and Storage Factors Affecting Acrylamide Formation in Processed Potatoes*. (Ph.D.). University of Minnesota, St. Paul, MN. Retrieved from <https://conservancy.umn.edu/handle/11299/190488>
- Sun, N., Y. Wang, S.K. Gupta, and C.J. Rosen. (2019). Nitrogen Fertility and Cultivar Effects on Potato Agronomic Properties and Acrylamide-Forming Potential. *Agron. J.*, 111(1), 408. <https://doi.org/10.2134/agronj2018.05.0350>.
- Sun, N., Y. Wang, S.K. Gupta, and C.J. Rosen. (2020). Potato Tuber Chemical Properties in Storage as Affected by Cultivar and Nitrogen Rate: Implications for Acrylamide Formation. *Foods*, 9(3). <https://doi.org/10.3390/foods9030352>.
- Thompson, A. (2013). 201300475. USDA PVPO.
- Thornton, M. (2020). Potato Growth and Development. In J. C. Stark, M. Thornton, and P. Nolte (Eds.), *Potato Production Systems* (pp. 19-33).
- Tiwari, J.K., D. Plett, T. Garnett, S.K. Chakrabarti, and R.K. Singh. (2018). Integrated Genomics, Physiology and Breeding Approaches for Improving Nitrogen Use Efficiency in Potato: Translating Knowledge from Other Crops. *Funct. Plant Biol.*, 45(6), 587. <https://doi.org/10.1071/fp17303>.
- USDA. (1997). United States Standards for Grades of Potatoes for Processing. Retrieved from [https://www.ams.usda.gov/sites/default/files/media/Potatoes\\_for\\_Processing\\_Standard%5B1%5D.pdf](https://www.ams.usda.gov/sites/default/files/media/Potatoes_for_Processing_Standard%5B1%5D.pdf)
- USDA NRCS. (2013). Soil Series Classification Database – Hubbard Series: United States Department of Agriculture. Retrieved from [https://soilseries.sc.egov.usda.gov/OSD\\_Docs/H/HUBBARD.html](https://soilseries.sc.egov.usda.gov/OSD_Docs/H/HUBBARD.html)
- Ushey, K. (2021). Renv: Project Environments. Retrieved from <https://CRAN.R-project.org/package=renv>
- Vander Zaag, P., A.L. Demagante, and E.E. Ewing. (1990). Influence of Plant Spacing on Potato (*Solanum Tuberosum* L.) Morphology, Growth and Yield under Two Contrasting Environments. *Potato Res.*, 33(313–323). <https://doi.org/10.1007/BF02359305>.
- Weather Spark. (2021). Compare the Climate and Weather in Becker, Saint-Léonard, Balcarce, and Gembloux. Retrieved from <https://weatherspark.com/compare/y/10443~27617~28950~51092/Comparison-of-the-Average-Weather-in-Becker-Saint-L%C3%A9onard-Balcarce-and-Gembloux>
- Wright, J. (2002). Irrigation Scheduling Checkbook Method. *BU-FO-01322*. St. Paul, MN: University of Minnesota. Retrieved from <https://extension.umn.edu/irrigation/irrigation-scheduling-checkbook-method>
- Yao, B., X. Wang, G. Lemaire, D. Makowski, Q. Cao, X. Liu, L. Liu, B. Liu, Y. Zhu, W. Cao, and L. Tang. (2021). Uncertainty Analysis of Critical Nitrogen Dilution Curves for Wheat. *Eur. J. Agron.*, 128, 126315. <https://doi.org/10.1016/j.eja.2021.126315>.



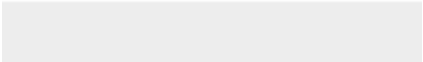

[Click here to access/download](#)

**Supplementary material for on-line publication only**  
bayesian-cndc-potato\_eja-submission\_supplement-  
v1.docx



[Click here to access/download](#)

**Supplementary material for on-line publication only**  
bayesian-cndc-potato\_eja-submission\_supplement-  
v1.xlsx



**Declaration of interests**

☐The authors declare that they have no known competing financial interests or personal relationships that could have appeared to influence the work reported in this paper.

☒The authors declare the following financial interests/personal relationships which may be considered as potential competing interests:

Carl J. Rosen reports financial support was provided by Minnesota Area II Potato Growers Research and Promotion Council.
--